A Renormalisation Group Approach to Graphene

A Thesis submitted for the completion of requirements for the degree of

Master of Science
(Research)

by

Biplab Mahato
Undergraduate Programme
Indian Institute of Science

Under the supervision of

Prof. H. R. Krishnamurthy
Indian Institute of Science

Prof. Subhro Bhattacharjee
International Center for Theoretical Sciences

Acknowledgement

I would like to thank the Undergraduate Program at Indian Institute of Science for providing an excellent environment which deepened my curiosity for research and science in general.

My whole hearted gratitude to Prof. Hulikal Ramaiengar Krishnamurthy for his guidance, encouragement and insightful discussions which made this thesis possible. I am grateful to Dr. Subhro Bhattacharjee for all the fruitful discussions, feedbacks and help.

My thanks to all the friends at IISc who made the work enjoyable and UG life so much more colourful.

Finally, I would like to thank my family for supporting me throughout the stay at IISc as well as during the lockdown due to Covid-19.

Abstract

Band structure of Graphene becomes gapless at the Dirac points where we see the signature of massless Dirac particles. In this thesis we try to describe Graphene near those point in the Renormalisation Group Framework. Perturbative Renormalisation Group methods are used to study two different interactions, Local interaction and Coulomb interaction upto one loop. As the relevant coupling constant α is more than unity, quantitatively accurate results are not expected from perturbative methods. So we look at the non-perturbative technique provided via Functional Renormalisation Group. Exact FRG equations are solved numerically to find the renormalisation of Fermi velocity and the dielectric function. We also extended the results to finite temperature and tried to include the frequency dependence in the interaction.

Contents

Introduction

Graphene has been a focus of research in condensed matter physics ever since its discovery. Easy access through experimentation and availability of a lot of exotic theoretical possibilities attracted a lot of minds. A huge amount of work both theoretically and experimentally has been done on various properties of graphene. A brief discussion about the existing literature on Graphene can be found in the excellent reviews by Castro Neto [1, 2].

The band structure of Graphene, within a tight binding framework that leads to two bands, was first derived by Wallace [3]. He also noticed that the band structure is gapless and near those points where the two bands touch each other, the theory becomes very similar to the massless Dirac theory. Since then many experiments have shown signatures of massless Dirac particles in Graphene [4]. If one adds in Coulomb type interaction then the theory resembles with $d = 2 + 1$ dimensional Quantum Electrodynamics (QED) with electron mass set to zero; with the exception that the speed of light is replaced by the Fermi velocity which is 300 times slower than c. This constitutes a boon as a lot of predictions of QED can be verified in this very accessible low energy system [5]. Since we are interested in the low energy behaviour, many have tried to find the low energy effective field theory starting from standard QED. The earliest work applying the Renormalisation Group to Graphene, dating back to 1993, is by Gonzalez et al [6]. They used dimensional regularization with $d = 3 - \epsilon$ to obtain leading order corrections to renormalisation factors. Later, many people have developed theories where the Coulomb interaction is treated as instantaneous. Shankar Das Sharma et al [7] have rederived all of those results and extended them to third order in[1] $\alpha = \frac{e^2}{v_F}$.

For graphene α is close to 2.2 hence a naive perturbative calculation should fail. Although the first order correction matches surprisingly well with the experimental data, Shankar Das Sharma showed that the second order corrections are not small and taking that into account does not agree with experiments. To go around this inconsistency, as shown by them, one should use renormalised interaction (from RPA calculation) instead of the bare Coulomb interaction. With this decent results were

[1] $\hbar$ is taken 1 throughout the text

obtained, and the results do not become worse after considering second order corrections. Even then it is not clear why perturbative expansion should be trusted as there is no sensible explanation of why first order theory agrees with experiments.

So naturally, we should look for some non-perturbative theory for Graphene. Functional Renormalisation Group(FRG) provides a way. Using this one can write a set of exact FRG equations [8]. These are set of coupled differential equations for various vertex functions, of which there are infinitely many in principle, which make their study really difficult. There are ways to close these equations by invoking approximations and obtain a finite number of coupled equations but even then it is very difficult to solve them analytically. Therefore one has to resort to numerical solutions. In a recent paper [9] by the group of Kopietz two coupled integro-differential equations are obtained which are solved numerically to obtain the velocity and the dielectric function. In this thesis, we develop and solve FRG equations for Graphene to reproduce earlier work as well as obtain some new results.

The thesis is organised as follows. The first two chapters are dedicated to setting up the basic ideas and theories. The first chapter defines the exact problem we are interested in and the second chapter sets up the path integral formalism for the theory. In the next two chapters, we use the perturbative RG to tackle Local and Coulomb interactions respectively. In the next chapter, we introduce the exact Functional Renormalisation Group equations and solve them numerically to reproduce the results in [9] as well as find some extension to it. Last two chapters are devoted to a discussion of some new results. The seventh chapter extends the results to finite temperature using Matsubara formalism and in the last chapter, we use several approximations to include the frequency dependence of the effective interaction taking inspiration from [10].

Chapter 1

Tight Binding Model

The chapter is dedicated to introducing the notations and formulate the problem under consideration.

1.1 Second Quantisation

Second Quantisation is a convenient language for describing many body quantum systems.

Suppose we want to describe a multi-particle quantum state. Axiomatically this can be done in the following way. First define a vacuum state $|\Omega\rangle$ which represents the state of the system in the absence of any particles whatsoever, much like the empty set in Set theory. Now we can construct any other state by having *particle creation operators* act on the vacuum state, which as the name suggests create particles in a given state or of given momentum depending on the choice of basis. Similarly we have the *annihilation operators*, which destroy particles. So a one particle state would be $|\psi_s\rangle = a_s^\dagger|\Omega\rangle$ where s carries the indices or labels(see the section below) that charecterise the created state. Correspondingly the annihilation of a two particle state gives a one particle state $a_1|\psi_1, \psi_2\rangle = |\psi_2\rangle$. Note that annihilation operator acting on the vacuum state should give zero $a_s|\Omega\rangle = 0 \forall s$. This uniquely defines the vacuum state. Finally we impose the condition that the operators follow the following relations

$$\{a_s, a_{s'}\} = \{a_s^\dagger, a_{s'}^\dagger\} = 0 \text{ and } \{a_s, a_{s'}^\dagger\} = \delta_{s,s'} \text{ for Fermions} \tag{1.1}$$

$$[a_s, a_{s'}] = [a_s^\dagger, a_{s'}^\dagger] = 0 \text{ and } [a_s, a_{s'}^\dagger] = \delta_{s,s'} \text{ for Bosons} \tag{1.2}$$

1.1.1 Representation and Basis

Two kinds of representation or the choice of basis will be used in this text. Firstly, consider a lattice of N points indexed by $i \in \{1, \ldots, N\}$, which has only one localised one particle state $|i\rangle$ at site i. Then we can represent the state of the system by the number of particles in each site i.e. $|\psi\rangle = |n_1, \ldots, n_N\rangle$ where n_i is the number of particles at site i. This is called the occupation number representation. In this notation then,

$$a_i^\dagger |n_1, \ldots, n_N\rangle = \sqrt{n_i + 1}|n_1, \ldots, n_i + 1, \ldots, n_N\rangle \tag{1.3}$$

$$a_i |n_1, \ldots, n_N\rangle = \sqrt{n_i}|n_1, \ldots, n_i - 1, \ldots, n_N\rangle \text{ or } 0 \text{ if } n_i = 0 \tag{1.4}$$

The normalisation constant are chosen to satisfy the (anti-)commutation relation in equations 1.1 and 1.2. Operators can be transformed into any other basis by using the resolution of identity. For example, we can write it in momentum space as follows,

$$a_{\boldsymbol{k}}^\dagger |\Omega\rangle = \sum_i \langle \boldsymbol{k}|i\rangle a_i^\dagger |\Omega\rangle \tag{1.5}$$

from where we can read off that,

$$a_{\boldsymbol{k}}^\dagger = \langle \boldsymbol{k}|i\rangle a_i^\dagger \tag{1.6}$$

$$a_{\boldsymbol{k}}^\dagger = \frac{1}{\sqrt{N}} \sum_i e^{-i\boldsymbol{k}.\boldsymbol{r}_i} a_i \tag{1.7}$$

Similar equations for the annihilation operators as well.

1.1.2 Single and Multi Particle Operator

Single and multi particle operators are the observables for the system. In the second quantisation formalism, we can write them easily. One particle operator (that change the state of a single particle) can be written as

$$\hat{\mathcal{O}}_1 = \sum_{i,j} \langle i|\mathcal{O}_1|j\rangle a_i^\dagger a_j \tag{1.8}$$

and two particle operators as

$$\hat{\mathcal{O}}_2 = \sum_{i,j,k,l} \langle i,j|\mathcal{O}_2|k,l\rangle a_i^\dagger a_j^\dagger a_k a_l \tag{1.9}$$

where $\langle i|\mathcal{O}_1|j\rangle$ is the matrix element which represents the overlap between the one

particle states $|i\rangle$ and $|j\rangle$ after it is acted upon by the operator $\mathcal{O}_1$ and so on.

1.2 Tight Binding Model Hamiltonian

For the tight binding model we first consider the non-interacting fermions where the Hamiltonian has a very simple form involving just one band with a dispersion $\mathcal{E}(\boldsymbol{k})$:

$$H_{free} = \sum_{\boldsymbol{k}} \mathcal{E}(\boldsymbol{k}) a^\dagger_{\boldsymbol{k}} a_{\boldsymbol{k}} \tag{1.10}$$

In position space this becomes

$$H_{free} = \frac{1}{N} \sum_{i,j} \sum_{\boldsymbol{k}} \mathcal{E}(\boldsymbol{k}) e^{i\boldsymbol{k}(\boldsymbol{r}_i - \boldsymbol{r}_j)} a^\dagger_i a_j \tag{1.11}$$

$$= \sum_{i,j} t_{ij} a^\dagger_i a_j \tag{1.12}$$

where we have defined $t_{ij} = \frac{1}{N} \sum_{\boldsymbol{k}} \mathcal{E}(\boldsymbol{k}) e^{i\boldsymbol{k}(\boldsymbol{r}_i - \boldsymbol{r}_j)}$. In the simplest version of this model we assume that the particles are so tightly attached to the lattice site that we only have hopping to the nearest sites. This is captured by a single parameter t called the hopping parameter ($t_{ij} = -t$ if i,j are nearest neighbour or else it is 0).

$$\boxed{H_{free} = -t \sum_{\langle i,j \rangle} (a^\dagger_i a_j + a^\dagger_j a_i)} \tag{1.13}$$

1.3 Graphene

In recent years graphene has been major focus area of condensed matter research. A single layer graphene's lattice looks like a honeycomb. Carbon atoms are placed on the vertices of hexagons with the spacing of ≈ 2.45 Åclosely knit together as shown in figure 1.1. Hexagonal lattice is not one of the Bravais lattices but is conveniently described as a combination of two triangular sublattices shifted from each other. These are shown in the figure as black and blue dots. These triangular lattices have a lattice spacing of $a = \sqrt{3} \times 2.45\text{Å} \approx 4.24$ Å

1.4 Band Structure

The second quantised tight binding Hamiltonian for graphene can be written as,

$$H = -t \sum_{\langle ij \rangle} c^\dagger_{i,A} c_{j,B} + \text{h.c} \tag{1.14}$$

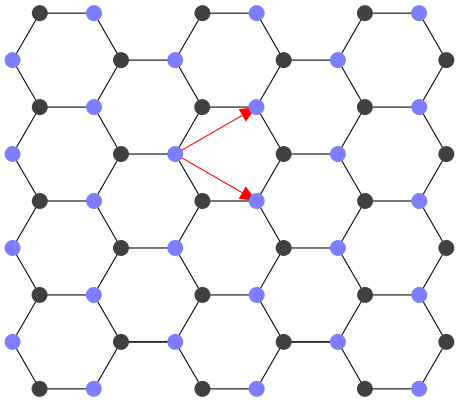

Figure 1.1: Graphene Lattice

where A and B label the two sublattices. Note that in the tight binding model hopping to the nearest neighbour has to involve a change in the sublattice index. Going into momentum space i.e. taking $c_{i,A/B} = \sum_{\boldsymbol{k}} c_{k,A/B} e^{i\boldsymbol{k}.\boldsymbol{R}_i}$ we have,

$$H = -t \sum_{\langle ij \rangle, \boldsymbol{k}, \boldsymbol{k'}} e^{-i\boldsymbol{k}.\boldsymbol{R}_i + i\boldsymbol{k'}.\boldsymbol{R}_j} c^{\dagger}_{\boldsymbol{k},A} c_{\boldsymbol{k'},B} + \text{h.c.} \tag{1.15}$$

$$= -t \sum_{i, \delta_j, \boldsymbol{k}, \boldsymbol{k'}} e^{-i(\boldsymbol{k}-\boldsymbol{k'}).\boldsymbol{R}_i} e^{i\boldsymbol{k'}.\boldsymbol{\delta}_j} c^{\dagger}_{\boldsymbol{k},A} c_{\boldsymbol{k'},B} + \text{h.c.} \tag{1.16}$$

where δ_j are the vectors specifying nearest neighbour. Summing over all the i coordinate we get a Kronecker delta which helps us to eliminate one of the momenta.

$$H = -t \sum_{\boldsymbol{k}, \boldsymbol{\delta}_j} e^{i\boldsymbol{k}.\boldsymbol{\delta}_j} c^{\dagger}_{\boldsymbol{k},A} c_{\boldsymbol{k},B} + e^{-i\boldsymbol{k}.\boldsymbol{\delta}_j} c^{\dagger}_{\boldsymbol{k},B} c_{\boldsymbol{k},A} \tag{1.17}$$

Hence we have block diagonalised the Hamiltonian into the different momentum channels. Now if we define the column vector $\psi(k) = (c_{\boldsymbol{k},A}, c_{\boldsymbol{k},B})^T$ we get,

$$H = \sum_{\boldsymbol{k}} \psi^{\dagger}(\boldsymbol{k}) h(\boldsymbol{k}) \psi(\boldsymbol{k}) \quad \text{where,} \quad h(\boldsymbol{k}) = t \begin{pmatrix} 0 & \sum_{\boldsymbol{\delta}_j} e^{i\boldsymbol{k}.\boldsymbol{\delta}_j} \\ \sum_{\boldsymbol{\delta}_j} e^{-i\boldsymbol{k}.\boldsymbol{\delta}_j} & 0 \end{pmatrix} \tag{1.18}$$

To get the eigenstates and the eigenenergies we need to diagonalise the matrix $h(\boldsymbol{k})$. Note that trace of the matrix is 0 which imply that the eigenvalues are $\pm\sqrt{det(h(\boldsymbol{k}))}$. Hence,

$$\mathcal{E}^{\pm}_{\boldsymbol{k}} = \pm t \sqrt{\left| \sum_{\boldsymbol{\delta}_j, \boldsymbol{\delta}_{j'}} e^{i\boldsymbol{k}.(\delta_{j'} - \delta_j)} \right|} \tag{1.19}$$

The nearest neighbours are situated at $\delta_1 = a(1,0)$, $\delta_2 = \frac{a}{2}(-1, \sqrt{3})$ and $\delta_3 = \frac{a}{2}(-1, -\sqrt{3})$. Substituting those in the above equation we get the dispersion relation

for the two bands as

$$\mathcal{E}^{\pm}_{\boldsymbol{k}} = \pm t\sqrt{3 + 4\cos(\frac{3ak_x}{2})\cos(\frac{\sqrt{3}ak_y}{2}) + 2\cos(\sqrt{3}ak_y)} \tag{1.20}$$

Figure 1.2 shows the above function inside the Brillouin Zone of graphene.

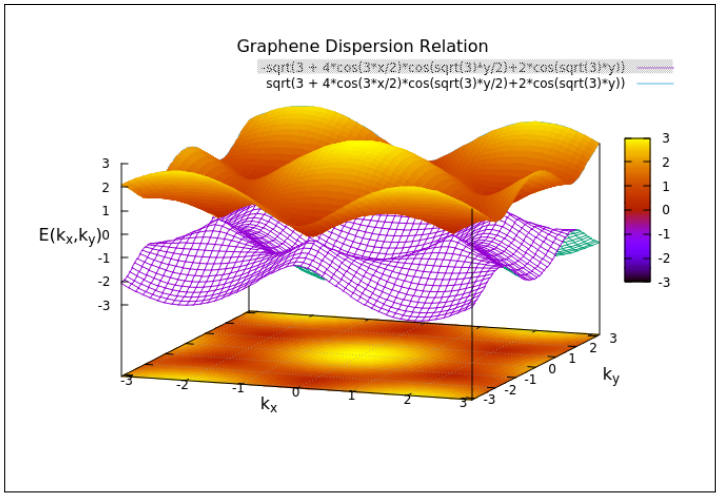

Figure 1.2: Band dispersions in Graphene as functions of momenta inside the Brillouin zone

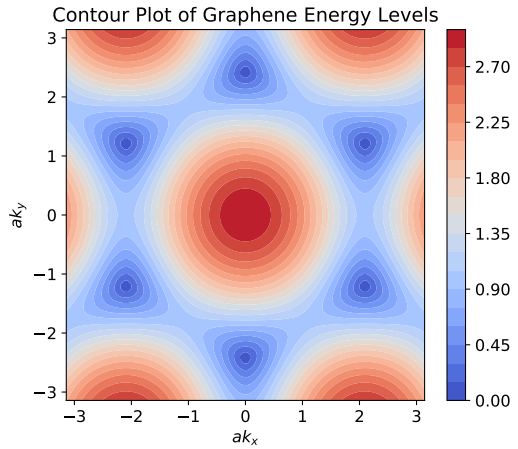

Figure 1.3: Contour Plot of the dispersion relation of Graphene for the lower, valence band. The upper, conduction band has exactly same contour plot with energy values having opposite sign

It is easy to see that there are **k** points where the determinant becomes zero then the gap between two bands vanishes at those points and system become gapless. The condition $\sum_{\delta_j} e^{i\boldsymbol{k}.\boldsymbol{\delta}_j} = 0$ is satisfied by two momenta $\boldsymbol{K}_1 = \frac{2\pi}{3a}(1, \frac{1}{\sqrt{3}})$ and $\boldsymbol{K}_2 = \frac{2\pi}{3a}(1, -\frac{1}{\sqrt{3}})$.

Expanding the matrix $h(\boldsymbol{k})$ near one of the point say $\boldsymbol{K}_1$ ($\boldsymbol{k} = \boldsymbol{K}_1 + \boldsymbol{q}$) gives

$$h(\boldsymbol{k}) = \begin{pmatrix} 0 & \sum_{\delta_j} e^{i\boldsymbol{K}_1.\boldsymbol{\delta}_j}(1 + i\boldsymbol{q}.\boldsymbol{\delta}_j) \\ \sum_{\delta_j} e^{-i\boldsymbol{K}_1.\boldsymbol{\delta}_j}(1 - i\boldsymbol{q}.\boldsymbol{\delta}_j) & 0 \end{pmatrix}$$

Substituting the values of δ_j's and $\boldsymbol{K}_1$ we get, $h(\boldsymbol{k}) = \frac{3}{2}at \begin{pmatrix} 0 & q_x + iq_y \\ q_x - iq_y & 0 \end{pmatrix} = \frac{3}{2}at\boldsymbol{\sigma}\cdot\boldsymbol{q}$. Similarly for the momenta near the momentum $\boldsymbol{K}_2$ we have $h(k) = -\frac{3}{2}at\boldsymbol{\sigma}^*\cdot\boldsymbol{q}$, where $\boldsymbol{\sigma}^* = (\sigma_x, -\sigma_y)$. So if we ignore the contribution from large values of $\boldsymbol{q}$ we can redefine the fields such that we have

$$H = v_F \sum_{\boldsymbol{q}} \Psi^\dagger_{1,\boldsymbol{q}}(\boldsymbol{q})\boldsymbol{\sigma}\cdot\boldsymbol{q}\Psi_{1,\boldsymbol{q}}(\boldsymbol{q}) + \Psi^\dagger_{2,\boldsymbol{q}}(q)(-\boldsymbol{\sigma}^*\cdot\boldsymbol{q})\Psi_{2,\boldsymbol{q}}(\boldsymbol{q}) \tag{1.21}$$

Here $v_F = \frac{3}{2}at$ is the Fermi Velocity (note in pristine Graphene. which has two electrons per unit cell, the Fermi level passes through $\boldsymbol{K}_1$ and $\boldsymbol{K}_2$)and $\Psi_{i,\boldsymbol{q}}(\boldsymbol{q}) = \psi(\boldsymbol{K}_i + \boldsymbol{q})$.

In the limit of small momentum $\boldsymbol{q}$ we can treat $\Psi_{1,\boldsymbol{q}}$ and $\Psi_{2,\boldsymbol{q}}$ as two independent fields. So, we have two uncoupled massless Dirac fields.

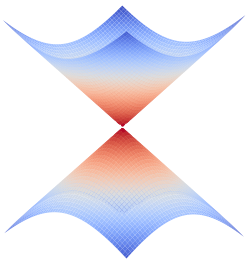

Figure 1.4: Dirac Cone

Chapter 2

Path Integral Formalism

2.1 Path Integral

Path integral was developed by Feynman to describe QED but since then it has been heavily used in almost all field theoretic (quantum many body) problems.

2.1.1 How to write Path Integral

In this section we review the basics of Path Integral Formalism following the discussion given in [11] and [12]. We start by noting that the time evolution operator given below provides a formal solution of the Schroedinger equation for a one electron Hamiltonian $\hat{H} = \hat{T} + \hat{V}$ where T and V are the kinetic and potential energy operators for a particle moving in one dimension.

$$U(t_f, t_i) = \theta(t_f - t_i) e^{-i\hat{H}(t_f - t_i)} \tag{2.1}$$

where the time evolution operator is defined by $|\psi(t_f)\rangle = U(t_f, t_i)|\psi(t_i)\rangle$ and the Heaviside theta function is there to respect causality.

It is hard to compute the exponential of a infinite dimensional operator for arbitrary time difference $(t_f - t_i)$. One way forward is to tackle the much simpler problem obtained by taking infinitesimally small time steps using the observation that

$$e^{-i\hat{H}(t_f - t_i)} = (e^{-i\hat{H}\Delta t})^N \tag{2.2}$$

where $\Delta t = \frac{t_f - t_i}{N}$.

Having a infinitesimal time step allows the simplification that

$$e^{-i\hat{H}\Delta t} = e^{-i\hat{T}\Delta t} e^{-i\hat{V}\Delta t} + O(\Delta t^2) \tag{2.3}$$

Using the above fact we can write the matrix element of the time development operator between initial and final position states

$$\langle q_f|(e^{-i\hat{H}\Delta t})^N|q_i\rangle = \langle q_f|\mathbf{1}e^{-i\hat{T}\Delta t}e^{-i\hat{V}\Delta t}\mathbf{1}\ldots\mathbf{1}e^{-i\hat{T}\Delta t}e^{-i\hat{V}\Delta t}|q_i\rangle \tag{2.4}$$

now we can introduce the following resolution of identity in the places wherever there is $\mathbf{1}$.

$$\int dq_n \int \frac{dp_n}{(\pi}|q_n\rangle\langle q_n|p_n\rangle\langle p_n| \tag{2.5}$$

where n runs from 1 to N. Realizing the fact that the operators act only on their eigenstates and using the relation $\langle q|p\rangle = e^{ipq}$ we have

$$\int \prod_{n=1}^{N} \frac{dq_n dp_n}{(2\pi)^D} e^{-i\Delta t \sum_{n=0}^{N-1}\left(V(q_n)+T(p_{n+1})-p_{n+1}\frac{q_{n+1}-q_n}{\Delta t}\right)} \tag{2.6}$$

Now if we take the limit $N \to \infty$ keeping $N\Delta t$ constant then the sum becomes an integral and $\frac{q_{n+1}-q_n}{\Delta t}$ can be identified with time derivative of position to finally obtain

$$\langle q_f|e^{-i\hat{H}(t_f-t_i)}|q_i\rangle = \int [Dx] e^{-i\int_{t_i}^{t_f} dt(H(p,q)-p\dot{q})} \tag{2.7}$$

where we have written the integration measure as $\int [Dx]$.

2.1.2 Fermionic Path integral

The previous section outlines the typical steps one takes in one particle Quantum Mechanics to set up a Path integral formulation. In Quantum Field theory/ Many body theory essentially same ideas go through with slight modifications. Position and momentum are replaced by fields which are functions of position. So from a normal path integration we go to functional integration. Also note that we need intermediate state similar to the position and momentum eigenstates. We have seen in previous chapters that the many body Hamiltonians are best written in terms of creation and annihilation operators (which are just linear combination of the fields). So we will look at the eigenstates of those operators. These are called *coherent states*, labeled by Grassmann numbers in case of Fermions. See appendix A for a brief discussion about them and their properties. Here we quote the two main results: resolution of

identity and the trace formula,

$$I = \int |\psi\rangle\langle\bar{\psi}| e^{-\bar{\psi}\psi} d\bar{\psi} d\psi \tag{2.8}$$

$$\text{Tr } \hat{\mathcal{O}} = \int \langle -\bar{\psi}|\hat{\mathcal{O}}|\psi\rangle e^{-\bar{\psi}\psi} d\bar{\psi} d\psi \tag{2.9}$$

As in Quantum Field Theory, evaluation of the n-point correlation functions are the most important quantities to calculate as they contain all the necessary information about the many body system. In a finite temperature setting, these averages are taken with respect to the quantum Gibbs probability distribution $\mathsf{p} = e^{-\beta\hat{H}}/\mathcal{Z}$. Here the quantum partition function is given by

$$\mathcal{Z} = \text{Tr } e^{-\beta\hat{H}} \tag{2.10}$$

Here we can use the trace formula stated earlier. Also we will adopt the approximation

$$e^{-\beta\hat{H}} = \lim_{N\to\infty} (e^{-\frac{\beta}{N}\hat{H}})^N \approx \underbrace{(1 - \tfrac{\beta}{N}\hat{H}) \dots (1 - \tfrac{\beta}{N}\hat{H})}_{N \text{ times}} \tag{2.11}$$

Using the trace formula and inserting resolution of identity $N-1$ times we arrive at

$$\begin{aligned}\mathcal{Z} = \int \langle -\bar{\psi}_1|1 - \tfrac{\beta}{N}\hat{H}|\psi_{N-1}\rangle e^{-\bar{\psi}_{N-1}\psi_{N-1}} \langle\bar{\psi}_{N-1}| \dots |\psi_2\rangle e^{-\bar{\psi}_2\psi_2} \\ \times \langle\bar{\psi}_2|(1 - \tfrac{\beta}{N}\hat{H})|\psi_1\rangle e^{-\bar{\psi}_1\psi_1} \prod_{n=1}^{N-1} d\bar{\psi}_n d\psi_n\end{aligned} \tag{2.12}$$

At this point we can simplify the expectation values inside the integral by noting that

$$\langle\bar{\psi}_{n+1}|1 - \tfrac{\beta}{N}\hat{H}(\Psi^\dagger, \Psi)|\psi_n\rangle = e^{\bar{\psi}_{n+1}\psi_n}(1 - \tfrac{\beta}{N}H(\bar{\psi}_{n+1}, \psi_n)) = e^{\bar{\psi}_{n+1}\psi_n} e^{-\frac{\beta}{N}H(\bar{\psi}_{n+1},\psi_n)}$$

where we have assumed that in the Hamiltonian the operators are already in the Normal order and the last step is only valid for large N. Using the above simplification we can finally write

$$\mathcal{Z} = \int \exp\left[\frac{\beta}{N}\sum_{n=1}^{N-1}\left(\frac{\bar{\psi}_{n+1} - \bar{\psi}_n}{(\beta/N)}\psi_n - H(\bar{\psi}_{n+1}, \psi_n)\right)\right] \prod_{n=1}^{N-1} d\bar{\psi}_n d\psi_n \tag{2.13}$$

where we have redefined $-\bar{\psi}_1$ as $\bar{\psi}_N$ to simplify the notation. In the limit $N \to \infty$ this becomes

$$\mathcal{Z} = \int_{\text{pbc}} e^{S[\bar{\psi},\psi]}[d\bar{\psi}d\psi], \quad S[\bar{\psi},\psi] = \int_0^\beta d\tau \left(\bar{\psi}\partial_\tau\psi - H(\bar{\psi},\psi)\right) \tag{2.14}$$

where the integration measure is written in square bracket. The discrete index n is replaced by continuous variable τ and the difference is identified with the derivative and used integration by parts to swap the derivative from $\bar{\psi}$ to ψ. Also note the periodic boundary condition coming from the definition $-\bar{\psi}_1 = \bar{\psi}_N$ as $\bar{\psi}(0) = -\bar{\psi}(\beta)$ and correspondingly $\psi(0) = -\psi(\beta)$. This allows us to write a discrete Fourier Transform for the integral in the action

$$\bar{\psi}(\tau) = \frac{1}{\beta}\sum_n e^{i\omega_n\tau}\bar{\psi}(\omega_n) \quad \text{and} \quad \psi(\tau) = \frac{1}{\beta}\sum_n e^{-i\omega_n\tau}\psi(\omega_n) \tag{2.15}$$

where to satisfy the boundary condition we must have $\omega_n = \frac{(2n+1)\pi}{\beta}$. These are called Matsubara Frequencies. We will only use them in the finite temperature chapter. Here we will work in zero temperature so we will take the $\beta \to \infty$ limit. In that limit sum over discrete Matsubara frequencies becomes an integral over a continuous variable ω

$$\mathcal{Z} = \int \exp\left[\int_{-\infty}^{\infty}\frac{d\omega}{2\pi}\left(\bar{\psi}(\omega)(i\omega)\psi(\omega) - H(\bar{\psi}(\omega),\psi(\omega))\right)\right][d\bar{\psi}(\omega)d\psi(\omega)] \tag{2.16}$$

Note that the Grassmann variables may depend on other indices like the momentum, spin etc. This can be easily seen by remembering that the creation and annihilation operators are indexed by momentum in the momentum representation like $\Psi^\dagger_{\mathbf{k}}$, which creates a particle with momentum $\mathbf{k}$. Then the corresponding Grassmann variables are also dependent on momenta and in the exponential those indexing variables need to be summed over or integrated out. To get a concrete example, consider the example we were working on i.e. graphene near Dirac points. In absence of any interaction terms, the Hamiltonian can be written as (see eqn 1.21)

$$\hat{H}(\Psi^\dagger,\Psi) = \sum_{i=1,2}\int\frac{d^2\mathbf{q}}{(2\pi)^2}\Psi^\dagger_{i,\mathbf{q}}(v_F\boldsymbol{\Sigma}_i.\mathbf{q})\Psi_{i,\mathbf{q}} \tag{2.17}$$

where $\{\boldsymbol{\Sigma_1}, \boldsymbol{\Sigma_2}\} = \{\boldsymbol{\sigma}, -\boldsymbol{\sigma}^*\}$. Then the partition function reads

$$\mathcal{Z} = \int \exp\left[\sum_{j=1,2}\int_{-\infty}^{\infty}\frac{d\omega}{2\pi}\int\frac{d^2\boldsymbol{q}}{(2\pi)^2}\bar{\psi}_j(\omega,\boldsymbol{q})(i\omega - v_F\boldsymbol{\Sigma_j}.\boldsymbol{q})\psi_j(\omega,\boldsymbol{q})\right][d\bar{\psi}(\omega,\boldsymbol{q})d\psi(\omega,\boldsymbol{q})] \tag{2.18}$$

As the two fields labeled by the Dirac cones does not interact with each other the partition function can be written as a multiplication of two separate partition functions $\mathcal{Z} = \prod_{j=1,2}\mathcal{Z}_j$.

2.2 Renormalization Group

Renormalization was the term originally used for the techniques which were invented to remove the infinities that arise in Quantum Electro-dynamics(QED) to get finite numbers as an end result. The techniques are often ad hoc but are very effective in producing experimentally verifiable quantities. Wilson approached the problem differently and came up with a different approach which is more physically intuitive and powerful. The techniques developed based on his ideas by himself and later by few others are known as Renormalization group techniques. This techniques usually start with a theory at high energies and iteratively go to theories at a smaller energies through a series of transformations. Lets consider a theory at some energy scale Λ written as $\boldsymbol{\mathcal{T}}_\Lambda$. Then a renormalization group transformation $\mathcal{R}(\Lambda', \Lambda)$ gives a theory at a different scale $\boldsymbol{\mathcal{T}}_{\Lambda'} = \mathcal{R}(\Lambda', \Lambda)\boldsymbol{\mathcal{T}}_\Lambda$. Note that we must always have $\Lambda' < \Lambda$ as theories with lower energy have lower number of degrees of freedom and creating a larger number of degrees of freedom from smaller numbers is ambiguous. Apart from that (nonexistence of inverse) the transformation follows all the properties of a mathematical group which is the origin for the name.

$$\mathcal{R}(\Lambda_1, \Lambda')\mathcal{R}(\Lambda', \Lambda_2) = \mathcal{R}(\Lambda_1, \Lambda_2) \qquad \text{(well defined product)}$$

$$\mathcal{R}(\Lambda_1, \Lambda_2)\left(\mathcal{R}(\Lambda_2, \Lambda_3)\mathcal{R}(\Lambda_3, \Lambda_4)\right) = \left(\mathcal{R}(\Lambda_1, \Lambda_2)\mathcal{R}(\Lambda_2, \Lambda_3)\right)\mathcal{R}(\Lambda_3, \Lambda_4) \quad \text{(associativity)}$$

The crucial step in a Wilsonian renormalization procedure involves 'integrating out' the higher energy degrees of freedom. For our case we will do it with momentum (others procedures are also possible). Let us write the fields as $\Psi_>$ and $\Psi_<$ to represent fields with momenta higher and lower than some cutoff Λ ($\Psi_> = \Psi_{|\boldsymbol{k}|>\Lambda}$, $\Psi_< = \Psi_{|\boldsymbol{k}|<\Lambda}$). And correspondingly, the Grassmanns $\psi_>$ and $\psi_<$. Then the partition function looks like

$$\mathcal{Z} = \int [d\bar{\psi}_> d\psi_> d\bar{\psi}_< d\psi_<] e^{S[\bar{\psi}_>, \psi_>; \bar{\psi}_<, \psi_<]} \tag{2.19}$$

The action can be written as

$$S[\bar{\psi}_>, \psi_>; \bar{\psi}_<, \psi_<] = S_0[\bar{\psi}_>, \psi_>] + S_0[\bar{\psi}_<, \psi_<] + S_I[\bar{\psi}_>, \psi_>; \bar{\psi}_<, \psi_<] \tag{2.20}$$

where the S_0 term only depends on the the momentum above or below the cutoff and the interaction term captures the cross-term. So then

$$\mathcal{Z} = \int [d\bar{\psi}_< d\psi_<] e^{S_0[\bar{\psi}_<, \psi_<]} \int [d\bar{\psi}_> d\psi_>] e^{S_0[\bar{\psi}_>, \psi_>]} e^{S_I[\bar{\psi}_>, \psi_>; \bar{\psi}_<, \psi_<]} \tag{2.21}$$

$$= \int [d\bar{\psi}_< d\psi_<] e^{S'[\bar{\psi}_<, \psi_<]} \tag{2.22}$$

where S' is the effective action after integrating out the higher momentum degrees of freedom.

The changes in the effective action after the RG procedure is the most interesting thing to look at. Although the comparison between effective action and the old action is ill defined as they have different set of arguments. In the latter, momentum can take values in $0 < k < \Lambda$ while if we have integrated out the momentum shell $\frac{\Lambda}{s} < k < \Lambda$ then effective action is only valid for momenta in $0 < k < \frac{\Lambda}{s}$. So to compare them one rescales the momenta by a factor of s. Rescaling of fields are also needed. This is done in such a way that the action of the free theory becomes a fixed point (action does not change under RG). After the rescaling one can compare the action by comparing the coefficients(real or complex) of each individual term in the action. The changes are represented in coefficient space where under RG it forms a trajectory. This is known as the flow of coefficients under RG. Relevant, irrelevant and marginal are terms used frequently for the coefficients which increases, decreases and remain same respectively under RG.

Depending on the interaction term the integral over the high momenta degree of freedom can be really daunting and for most cases impossible to do exactly. So we will use perturbation theory to do the integral.

2.3 Perturbation Theory and Feynman Diagrams

To evaluate the effective action we write

$$e^{S'[\bar{\psi}_<,\psi_<]} = e^{S_0[\bar{\psi}_<,\psi_<]} \frac{\int [d\bar{\psi}_> d\psi_>] e^{S_0[\bar{\psi}_>,\psi_>]} e^{S_I[\bar{\psi}_>,\psi_>;\bar{\psi}_<,\psi_<]}}{\int [d\bar{\psi}_> d\psi_>] e^{S_0[\bar{\psi}_>,\psi_>]}} \mathcal{Z}_{0>} \tag{2.23}$$

Now the middle portion of the right hand side represent the expectation value of $e^{S_I[\bar{\psi}_>,\psi_>;\bar{\psi}_<,\psi_<]}$ with respect to only the high momenta. Also note that $\mathcal{Z}_{0>}$ can be dropped as it will only add a constant term to the partition function.

To handle the complicated expectation value we will use the cumulant expansion

$$\langle e^{\Omega} \rangle = e^{\sum_{n=1}^{\infty} c_n/n!} = e^{\left(\langle\Omega\rangle + \left(\langle\Omega^2\rangle - \langle\Omega\rangle^2\right)/2 + \ldots\right)} \tag{2.24}$$

where we have written the cumulants in terms of the moments upto second order. The terms to be averaged are product of monomials in the Grassmaans. The higher momenta Grassmann's are to be averaged over. We can use the Wick's theorem here and be left with just one type of averaging namely

$$\langle \bar{\psi}_> \psi_> \rangle = \frac{\int [d\bar{\psi}_> d\psi_>] \bar{\psi}_> \psi_> e^{S_0[\bar{\psi}_>,\psi_>]}}{\int [d\bar{\psi}_> d\psi_>] e^{S_0[\bar{\psi}_>,\psi_>]}} \tag{2.25}$$

which for the case of graphene i.e. the action used in the partition function given in eqn 2.18 and using the integral given in appendix A.10 evaluates to

$$\langle \bar{\psi}_i(\omega_1, \boldsymbol{k}_1)\psi_j(\omega_2, \boldsymbol{k}_2)\rangle = \delta_{ij}\delta(\omega_1 - \omega_2)\delta(\boldsymbol{k}_1 - \boldsymbol{k}_2)\frac{1}{i\omega - v_F \boldsymbol{\Sigma}_j \cdot \boldsymbol{k}_1} =: G_j^{(0)}(i\omega, \boldsymbol{k}_1) \quad (2.26)$$

As an example how this works lets take the instantaneous local interaction with four operators i.e. $S_I = V\bar{\psi}_\alpha\bar{\psi}_\beta\psi_\gamma\psi_\delta$ where the Greek indices carry the labels. There are various possibilities at this point ψ's can have momenta higher or lower than the cutoff. If all four of them have higher momenta then it would just add a constant term in the partition function hence can be ignored. If there are odd number of high momenta then the term vanishes by symmetry. So we are left with two types of terms one with all momenta lower than the cutoff which can be added to the effective action without any change and the other terms with equal number of high and low momenta. In the latter terms we can use the above averaging formula to simplify and then integrate out the higher momenta. The combinatorics here can be simplified by using Feynman diagrams to represent the different terms. The fields are shown as lines and S_I gives the vertex. For example, in case of the interaction above we have four lines joining a vertex. The fields which are not averaged i.e. the slow modes constitute the external lines and the averaged fields are the internal lines. These are exactly like the Feynman diagrams that are used in the Quantum Field Theory except that only the fast modes constitutes the internal lines and they are to be integrated out. One more thing to note is that in the second cumulant the $-\langle\Omega\rangle^2$ removes the disconnected Feynman diagram (the diagram with two disconnected lines). Similarly we can see that we are supposed to write all disconnected diagrams possible up to some order and carry out our calculations.

Chapter 3

One loop calculations

Interactions are the soul of Physics. In this chapter we will introduce the interactions that are used in the text.

Two particle interaction in full generality (without spin) have the following form,

$$\sum_{iji'j'\in\{1,2\}} \sum_{\boldsymbol{k}_1,\boldsymbol{k}_2,\boldsymbol{k}_3,\boldsymbol{k}_4} V_{iji'j'}(\boldsymbol{k}_1,\boldsymbol{k}_2,\boldsymbol{k}_3,\boldsymbol{k}_4)\Psi^\dagger_{i,\boldsymbol{k}_1}(\boldsymbol{k}_1)\Psi^\dagger_{j,\boldsymbol{k}_2}(\boldsymbol{k}_2)\Psi_{i',\boldsymbol{k}_3}(\boldsymbol{k}_3)\Psi_{j',\boldsymbol{k}_4}(\boldsymbol{k}_4) \tag{3.1}$$

with an overall momentum conservation.

Two types of interaction will be treated.

- **Local Interaction** $V_{iji'j'}$ does not depend on any momentum which is equivalent to zeroth component of the Taylor expansion of the interaction with respect to the momenta. In RG term this is the only relevant coefficient of such expansion.
- **Coulomb Interaction** $\frac{e^2}{r}$ type of interaction in position space. In 2d, momentum space form of the interaction is $V(\boldsymbol{q}) = \frac{2\pi e^2}{q}$. We treat this interaction in the next chapter.

3.1 Local Interaction

The interaction have the form

$$\sum_{iji'j'\in\{1,2\}} V_{iji'j'}\Psi^\dagger_{i,\boldsymbol{k}_1}(\boldsymbol{k}_1)\Psi^\dagger_{j,\boldsymbol{k}_2}(\boldsymbol{k}_2)\Psi_{i',\boldsymbol{k}_3}(\boldsymbol{k}_3)\Psi_{j',\boldsymbol{k}_4}(\boldsymbol{k}_4) \tag{3.2}$$

with the overall delta function for the momentum conservation as below

$$\delta\left((\boldsymbol{K}_i+\boldsymbol{k}_1)+(\boldsymbol{K}_j+\boldsymbol{k}_2)-(\boldsymbol{K}_{i'}+\boldsymbol{k}_3)-(\boldsymbol{K}_{j'}+\boldsymbol{k}_4)\right) \tag{3.3}$$

Note that $\boldsymbol{K}_i$'s should cancel each other to avoid problems in the momentum rescaling process. Which will leave us with the possibilities that either all the indices are same or both i and j are different in that case i' and j' are also required to be different. Consider the first possibility

$$V_{1111}\Psi^\dagger_{1,\boldsymbol{k}_1}(\boldsymbol{k}_1)\Psi^\dagger_{1,\boldsymbol{k}_2}(\boldsymbol{k}_2)\Psi_{1,\boldsymbol{k}_3}(\boldsymbol{k}_3)\Psi_{1,\boldsymbol{k}_4}(\boldsymbol{k}_4) + V_{2222}\Psi^\dagger_{2,\boldsymbol{k}_1}(\boldsymbol{k}_1)\Psi^\dagger_{2,\boldsymbol{k}_2}(\boldsymbol{k}_2)\Psi_{2,\boldsymbol{k}_3}(\boldsymbol{k}_3)\Psi_{2,\boldsymbol{k}_4}(\boldsymbol{k}_4) \tag{3.4}$$

In our theory we will not break the symmetry between the valleys, hence we take $V_{1111} = V_{2222} =: \frac{U}{2!2!}$. The second possibility

$$\frac{V}{2!2!}\Psi^\dagger_{1,k_4}\Psi^\dagger_{2,k_3}\Psi_{2,k_2}\Psi_{1,k_1} + \frac{V}{2!2!}\Psi^\dagger_{2,k_4}\Psi^\dagger_{1,k_3}\Psi_{1,k_2}\Psi_{2,k_1} \tag{3.5}$$

where we have taken $V_{1221} = V_{2112} =: \frac{V}{2!2!}$.

Feynman diagrams for this theory, are given in figure 3.1 where we have used solid and dashed line to distinguish propagators of different valleys.

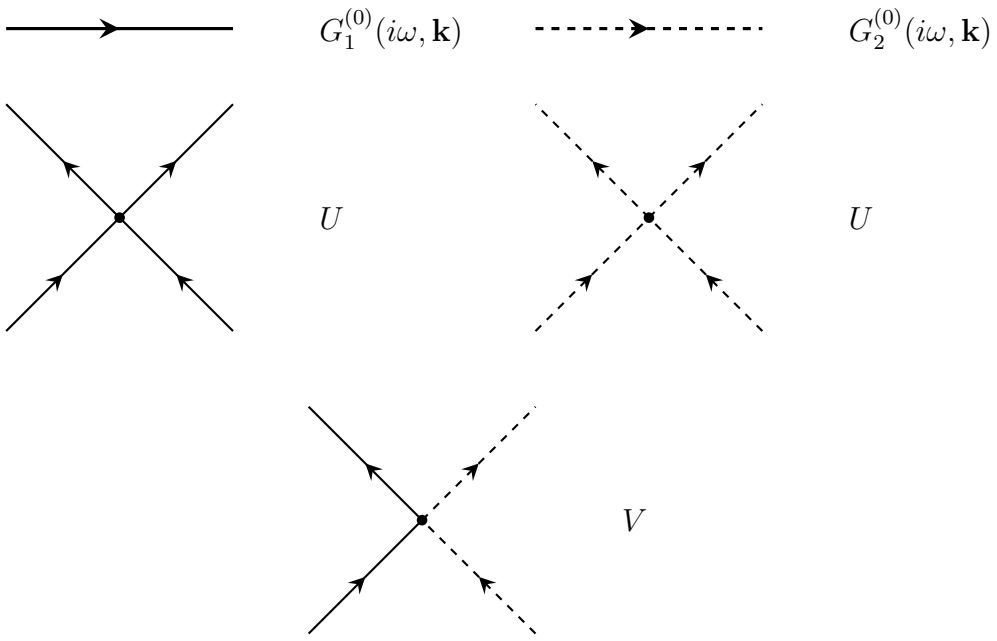

Figure 3.1: Feynman Diagrams for the local interaction. Solid and dashed line represent propagators of two different valleys

3.1.1 Renormalisation of Two point Function

The connected Feynman diagrams that renormalise the two point function are in fig 3.2.

All the tadpole diagrams in the fig 3.2 evaluate to the same upto a factor. For example the diagram (a) translates to

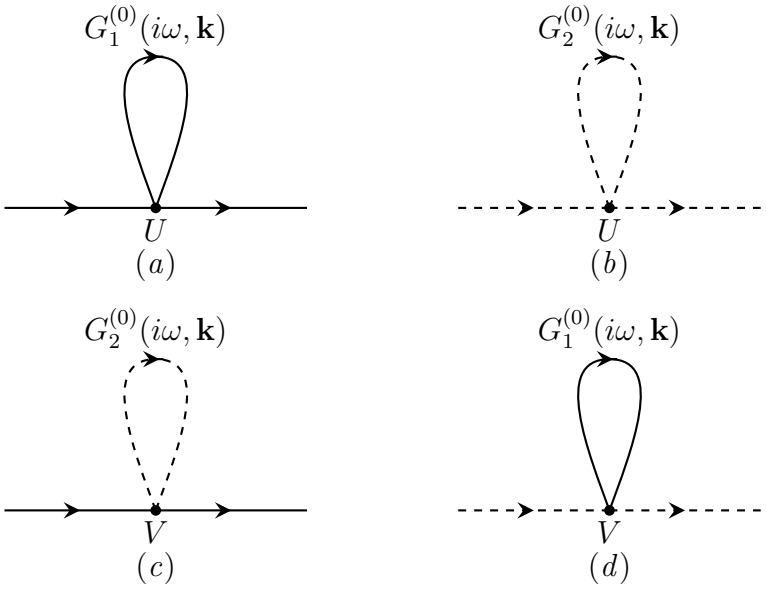

Figure 3.2: Tadpole Diagrams. (a) and (c) renormalise the propagator of the first valley, (b) and (d) the other valley

$$U \int_{-\infty}^{\infty} \frac{d\omega}{2\pi} \int_{\frac{\Lambda}{s}<|k|<\Lambda} \frac{d^2k}{(2\pi)^2} G_1^{(0)}(i\omega, k) \tag{3.6}$$

We will evaluate the ω integral first. The poles are at $\pm i v_F|k|$. We can close the loop on either side to get contribution from only one of the pole. For example lets close the loop on the upper half complexplane to get.

$$U \int_{\frac{\Lambda}{s}<|k|<\Lambda} \frac{d^2k}{(2\pi)^2} \frac{v_F|k| + v_F \boldsymbol{\sigma} \cdot \boldsymbol{k}}{2v_F|k|} = U \int_{\frac{\Lambda}{s}<|k|<\Lambda} \frac{d^2k}{(2\pi)^2} \frac{1}{2} \left(1 + \frac{\boldsymbol{\sigma} \cdot \boldsymbol{k}}{|k|}\right) \tag{3.7}$$

The $\boldsymbol{\sigma} \cdot \boldsymbol{k}$ part vanishes as it is an odd function of k. The other part gives

$$U \int_{\frac{\Lambda}{s}}^{\Lambda} \frac{2\pi k dk}{(2\pi)^2} \frac{1}{2} = \frac{U\Lambda^2}{8\pi} \left(1 - \frac{1}{s^2}\right) \tag{3.8}$$

Similarly, the diagram (c) evaluates to $\frac{V\Lambda^2}{8\pi}\left(1 - \frac{1}{s^2}\right)$. Note that both of these are proportional to identity hence generate chemical potential like term in the effective action.

3.1.2 Renormalisation of Interaction Vertex

For the renormalisation of the interaction vertices U and V at one loop, we have the following diagrams 3.3. Top(bottom) four diagrams renormalise $U(V)$. Each diagram can be of three types ZS, ZS', and BCS depending on their topology as

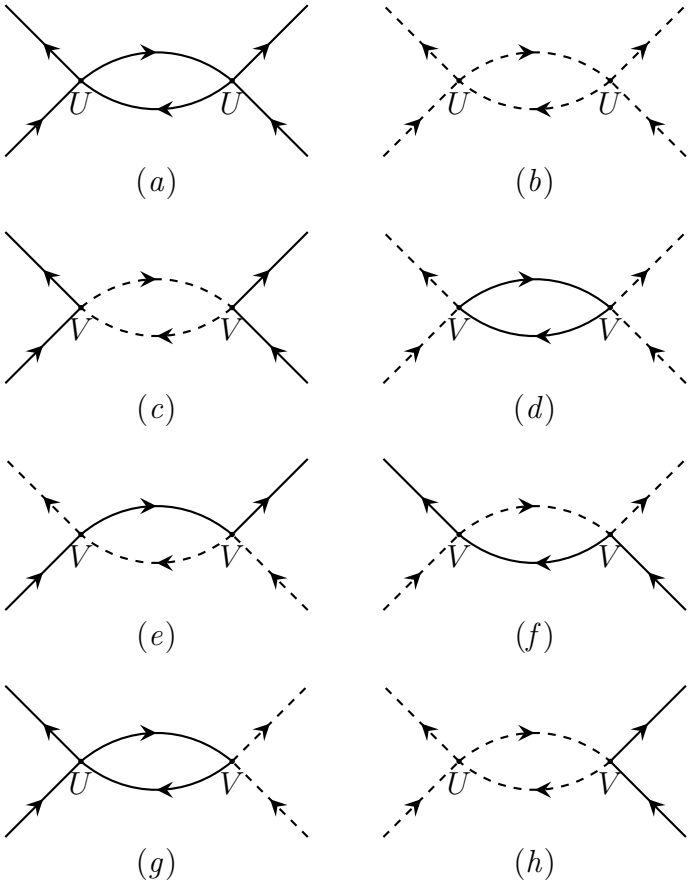

Figure 3.3: One loop correction to the Couplings. Subfigures (a-d) renormalise the intra-valley interaction while subfigures (e-h) renormalise the inter-valley interaction

shown in fig 3.4

Intra-valley

First consider the renormalisation of U i.e. the top four figure in 3.3. They all have the same form (upto a factor)

$$U^2 \int_{-\infty}^{\infty} \frac{d\omega_5 d\omega_6}{(2\pi)^2} \int_{\frac{\Lambda}{s}<k_5,k_6<\Lambda} \frac{d^2\boldsymbol{k}_5 d^2\boldsymbol{k}_6}{(2\pi)^4} G_1^{(0)}(i\omega_5, \boldsymbol{k}_5) G_1^{(0)}(i\omega_6, \boldsymbol{k}_6) \tag{3.9}$$

Overall delta function for the momentum conservation at each vertex also fixes the relation between $\boldsymbol{k}_5$ and $\boldsymbol{k}_6$.

- **ZS:** $\boldsymbol{k}_5 - \boldsymbol{k}_6 = \boldsymbol{k}_1 - \boldsymbol{k}_4$
- **ZS′** : $\boldsymbol{k}_5 - \boldsymbol{k}_6 = \boldsymbol{k}_1 - \boldsymbol{k}_3$
- **BCS:** $\boldsymbol{k}_5 + \boldsymbol{k}_6 = \boldsymbol{k}_1 + \boldsymbol{k}_2$

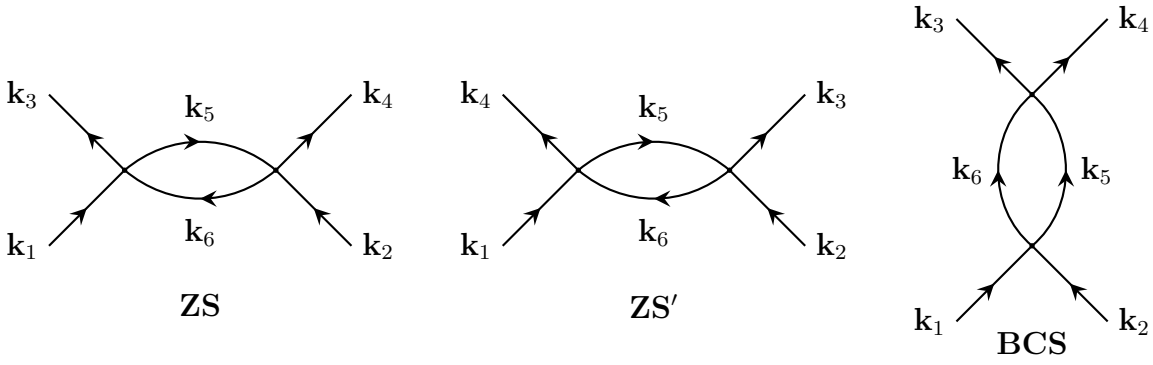

Figure 3.4: Three types of diagrams depending on the topology of the graph

and similar equation for the frequencies. For the calculation of β function we can set the external momenta and frequencies to be zero. This means that we have $\boldsymbol{k}_5 = \boldsymbol{k}_6$ and $\omega_5 = \omega_6$ for ZS and ZS' diagrams while $\boldsymbol{k}_6 = -\boldsymbol{k}_5$ and $\omega_6 = -\omega_5$ for BCS diagram. In all the cases we are supposed to calculate the same integral as in BCS diagram both frequency and momentum change sign contributing an overall minus sign. To calculate the integral we will rewrite the propagator in a different form (chiral representation)

$$G_1^{(0)}(i\omega, \boldsymbol{k}) = \sum_{s=\pm 1} \frac{1}{2} \frac{1 + s\frac{\boldsymbol{\sigma}\cdot\boldsymbol{k}}{k}}{i\omega - sv_F k} \tag{3.10}$$

So we get two kind of terms in 3.9. One with both the factors in the denominator having same sign of s's and the other having opposite signs. For the terms having same sign, the integrand have pole on one half of the complex plane and so we can always close the contour on the other side to get zero. For the case when the factors have opposite signs of s's, we have the integrand

$$\frac{1}{4} \frac{(1 + \frac{\boldsymbol{\sigma}\cdot\boldsymbol{k}}{k})(1 - \frac{\boldsymbol{\sigma}\cdot\boldsymbol{k}}{k})}{(i\omega - v_F k)(i\omega + v_F k)} = \frac{1}{4} \frac{1 - \frac{(\boldsymbol{\sigma}\cdot\boldsymbol{k})(\boldsymbol{\sigma}\cdot\boldsymbol{k})}{k^2}}{(i\omega - v_F k)(i\omega + v_F k)} \tag{3.11}$$

The numerator vanishes as $(\boldsymbol{\sigma}\cdot\boldsymbol{k})(\boldsymbol{\sigma}\cdot\boldsymbol{k}) = k^2$. So all the diagrams vanish.

Therefore we do not have any renormalisation for the vertex U at one loop.

Inter-valley

Next we look at the renormalisation of V i.e. the bottom four diagrams in fig 3.3. Last two diagrams vanish as they are identical to the 3.9. The remaining two diagrams have propagators from both the valleys in the integrand

$$V^2 \int_{-\infty}^{\infty} \frac{d\omega_5 d\omega_6}{(2\pi)^2} \int_{\frac{\Lambda}{s} < |k_5|, |k_6| < \Lambda} \frac{d^2k_5 d^2k_6}{(2\pi)^4} G_1^{(0)}(i\omega_5, k_5) G_2^{(0)}(i\omega_6, k_6) \tag{3.12}$$

relation between $\boldsymbol{k}_5$ and $\boldsymbol{k}_6$ turns out to be same as previous ones $\boldsymbol{k}_6 = \boldsymbol{k}_5$ for ZS and ZS' and $\boldsymbol{k}_6 = -\boldsymbol{k}_5$ for BCS. Lets focus on one of the integrals (the other integral is also same with an overall sign). We can again use the similar chiral representation of $G_2^{(0)}$

$$G_2^{(0)}(i\omega, \boldsymbol{k}) = \sum_{s=\pm 1} \frac{1}{2} \frac{1 + s\frac{\boldsymbol{\sigma^*}\cdot\boldsymbol{k}}{k}}{i\omega + sv_F k} \tag{3.13}$$

Note that the denominator of both $G_1^{(0)}$ and $G_2^{(0)}$ are of the same form. So following the arguments encountered in evaluating eqn 3.9, we only have the cross terms. Both the cross terms are exactly same and equal to

$$V^2 \int_{-\infty}^{\infty} \frac{d\omega}{2\pi} \int_{\frac{\Lambda}{s}<k<\Lambda} \frac{d^2k}{(2\pi)^2} \frac{1}{4} \frac{1 - \frac{(\boldsymbol{\sigma}\cdot\boldsymbol{k})(\boldsymbol{\sigma^*}\cdot\boldsymbol{k})}{k^2}}{(i\omega - v_F k)(i\omega + v_F k)} \tag{3.14}$$

The numerator becomes $\left(1 - \frac{k_1^2 - k_2^2}{k_1^2 + k_2^2}\right) = \frac{2k_2^2}{k_1^2 + k_2^2}$ where k_1 and k_2 are the components of the two dimensional momentum vector k. We can replace k_2^2 with $\frac{1}{2}(k_1^2 + k_2^2)$, which will make the numerator unity. ω integral can be done by taking a contour closing on the upper half of the complex plane to get

$$V^2 \int_{\frac{\Lambda}{s}<k<\Lambda} \frac{d^2k}{(2\pi)^2} \frac{1}{4} \frac{1}{2v_F k} = V^2 \int_{\frac{\Lambda}{s}}^{\Lambda} \frac{2\pi k dk}{(2\pi)^2} \frac{1}{4} \frac{1}{2v_F k} = \frac{V^2}{16\pi v_F} \left(\Lambda - \frac{\Lambda}{s}\right) \tag{3.15}$$

So these two terms together contribute $\frac{V^2\Lambda}{8\pi v_F}\left(1 - \frac{1}{s}\right)$.

3.1.3 Recursion Relations

Now that we have calculated all the Feynman diagrams at one loop we can write the recursion relations for the RG.

- Fermi velocity does not renormalise at one loop.
- Chemical potential increases as

$$\mu' = s\left(\mu + \frac{(U+V)\Lambda^2}{8\pi}\left(1 - \frac{1}{s^2}\right)\right) \tag{3.16}$$

- The interaction term U does not renormalises at one loop
- The interaction controlling the inter-valley scattering renormalises as (Note $ZS' = -BCS$)

$$V' = V - ZS' - \frac{1}{2}BCS = V - \frac{1}{2}\frac{V^2\Lambda}{8\pi v_F}\left(1 - \frac{1}{s}\right) \tag{3.17}$$

The recursion relations show that as we carry out the Renormalisation process Fermi velocity v_F and the intra-valley interaction U does not change while the chemical potential (which was zero initially) keeps increasing and the inter-valley interaction V decreases.

Chapter 4

Hubbard Stratonovich Transformation

4.1 Theory

Hubbard-Stratonovitch transformation is one of the tricks which is very often used in condensed matter physics. It introduces auxiliary fields into the picture to decouple fields and get a simpler form of the action to work with.

Note that, the interaction terms in case of fermions are quartic in fields. This makes the evaluation of (Grassmann) functional integrals with such terms in the action much more difficult compared to free theories. In case of local interaction perturbative RG equations to leading orders are derivable but for an arbitrary interaction potential, for example the Coulomb interaction, any explicit calculation becomes very difficult. To overcome this, we will use the following route provided by Hubbard and Stratonovitch.

First note that the action we are working with in the case of Coulomb interaction is

$$S[\bar{\psi},\psi] = \sum_K \bar{\psi}_K \left(-i\omega + \varepsilon(\mathbf{k})\right)\psi_K + \frac{1}{2!2!}\sum_{KK'Q} \bar{\psi}_{K+Q}\bar{\psi}_{K'-Q}V(\mathbf{q})\psi_{K'}\psi_K \tag{4.1}$$

where we have used a compact notation $K = (i\omega, \boldsymbol{k})$ and $V(\boldsymbol{q}) = \frac{2\pi e^2}{q}$. Also, let us define the density operator as $\rho_Q = \sum_K \bar{\psi}_K\psi_{K+Q}$ which will enable us to write the interaction term as $\sum_Q \rho_Q V(\mathbf{q})\rho_{-Q}$. Now we can introduce a real Bosonic field in a form of unity and insert the unity in the partition function expression.

$$\mathbf{1} = \int [D\phi] \exp\left[-e^2 \sum_Q \phi_Q V^{-1}(\boldsymbol{q})\phi_{-Q}\right] \tag{4.2}$$

where we have absorbed a normalisation factor into the integration measure. And the e^2 factor to cancel out the e^2 factor present in the interaction. Now if we shift the field ϕ_Q to $\phi_Q + \frac{ie}{2}V(\boldsymbol{q})\rho_Q$ to get

$$\mathbf{1} = \int [D\phi] \exp\left[\sum_Q -e^2\phi_Q V^{-1}(\boldsymbol{q})\phi_{-Q} - ie\rho_Q\phi_{-Q} + \frac{1}{4}\rho_Q V(\boldsymbol{q})\rho_{-Q}\right] \tag{4.3}$$

Substituting this into the partition function cancels the last term and we obtain

$$S[\bar{\psi},\psi,\phi] = \sum_K \bar{\psi}_K(-i\omega + \varepsilon(\boldsymbol{k}))\psi_K + e^2\sum_Q \phi_Q V^{-1}(\boldsymbol{q})\phi_{-Q} + ie\sum_{K,Q}\bar{\psi}_K\phi_Q\psi_{K+Q} \tag{4.4}$$

The first two terms are in the form of quadraic action of free theories. They produce two propagators one for the fermion and one for the auxiliary Bosonic field. For the case of graphene with spinless electrons this auxiliary field is a real Bosonic field with no indices. Then the propagators are $(i\omega - \boldsymbol{\sigma}.\boldsymbol{p})^{-1}$ and $\frac{2\pi}{q}$ respectively. Finally the last term gives the coupling between these two terms. The Feynman diagrams corresponding to the propagators and vertex of the action are shown in figure 4.1.

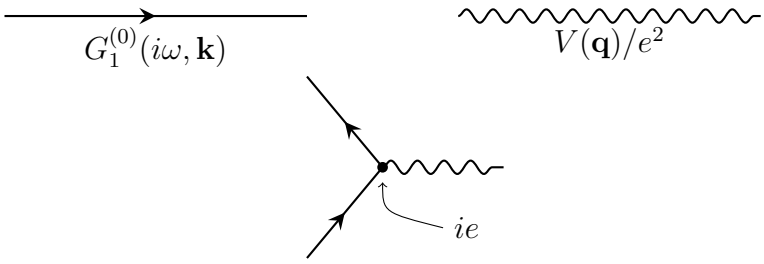

Figure 4.1: Feynman Diagrams for the Hubbard Stratonovitch transformed fields

4.2 Calculations

4.2.1 Self Energy

We can now use Feynman diagrams to calculate the correction terms to the free theory due to the interaction. For example, the following two diagrams shown in fig 4.2 give the one loop self energy corrections to the electron propagator. The first diagram translates to

$$\int_{K=(i\omega,\boldsymbol{k})} \frac{d^3K}{(2\pi)^3} V(0)G^{(0)}(i\omega,\boldsymbol{k}) \tag{4.5}$$

One might interject that $V(0)$ is not defined or finite, unless one uses the renormlaised or dressed Coulomb interaction results in a finite value of $V(0)$. Moreover, this term gets canceled by the contribution from the neutrilising positive charge.

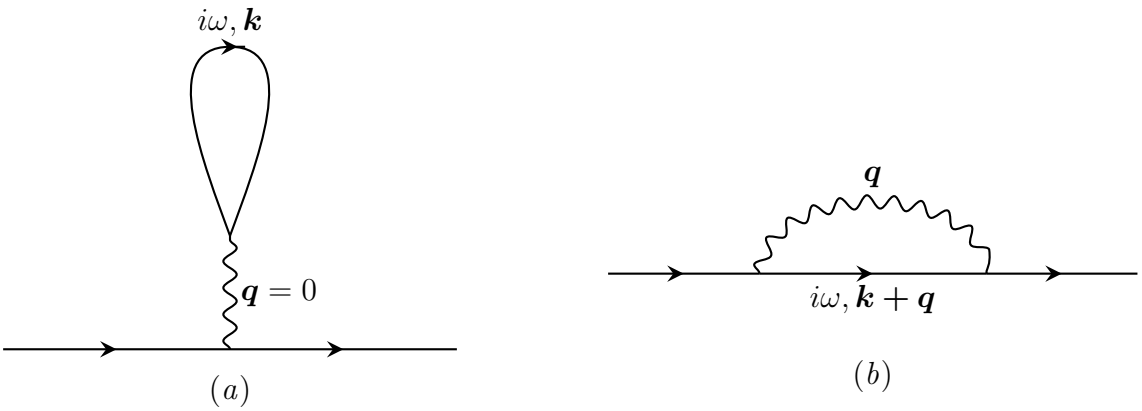

Figure 4.2: Feynman Diagram at one loop

From the diagram (b) in 4.2 we get

$$\Sigma(\boldsymbol{k}) = \int_{Q=(i\omega,\boldsymbol{q})} \frac{d^3Q}{(2\pi)^3} V(q) G^{(0)}(i\omega, \boldsymbol{k}+\boldsymbol{q}) \tag{4.6}$$

Since the interaction term does not have a frequency dependence, the frequency integral can be easily done to have

$$\int_{\boldsymbol{q}} \frac{d^2\boldsymbol{q}}{(2\pi)^2} \frac{2\pi e^2}{q} \frac{1}{2} \left(1 + \frac{\boldsymbol{\sigma}.(\boldsymbol{k}+\boldsymbol{q})}{|\boldsymbol{k}+\boldsymbol{q}|}\right) \tag{4.7}$$

Where we need to integrate out the momentum which satisfy $\frac{\Lambda}{s} < q < \Lambda$ and $\frac{\Lambda}{s} < |\boldsymbol{k}+\boldsymbol{q}| < \Lambda$. To be able to do the integral we will use a substitution which will let us do most of the integrals in this text. Firstly we take $\boldsymbol{k} = (k, 0)$ and

$$\boldsymbol{q} = \frac{k}{2}\left(1 - \cosh(\mu)\cos(\nu), \sinh(\mu)\sin(\nu)\right) \tag{4.8}$$

This means the Jacobian is $\frac{1}{8}k^2(\cosh(2\mu) - \cos(2\nu)) = \frac{1}{4}k^2(\cosh^2\mu - \cos^2\nu)$ and $q = \frac{k}{2}(\cosh\mu - \cos\nu)$, $|\boldsymbol{k}+\boldsymbol{q}| = \frac{k}{2}(\cosh\mu + \cos\nu)$. So clearly with this substitution we are able cancel out the q and $|\boldsymbol{k}+\boldsymbol{q}|$ in the denominator. Also the in shell condition becomes $\frac{\Lambda}{s} < \frac{k}{2}(\cosh\mu \pm \cos\nu) < \Lambda$.

In the integrand the first term gives rise to a term corresponding to the identity which gives a chemical potential like term. For the other part we have

$$\int_0^{2\pi} \frac{e^2 d\nu}{4\pi} \int_{\mu_{\min}}^{\mu_{\max}} d\mu \boldsymbol{\sigma}.(\boldsymbol{k}+\boldsymbol{q}) = \int_0^{2\pi} \frac{d\nu}{4\pi} \int_{\mu_{\min}}^{\mu_{\max}} d\mu \frac{k}{2} \left(\sigma_1(1 + \cosh\mu\cos\nu) + \sigma_2 \sinh\mu\sin\nu\right)$$

Where we have introduced $\mu_{\min} = \cosh^{-1}\left(\frac{2\Lambda}{ks} + |\cos\nu|\right)$ and $\mu_{\max} = \cosh^{-1}\left(\frac{2\Lambda}{k} - |\cos\nu|\right)$ to satisfy the in shell condition. Then it is easy to see that the terms with $\sin\nu$ and

$\cos\nu$ as a factor vanishes. So then

$$\int_0^{2\pi} \frac{e^2 d\nu}{8\pi} k\sigma_1 \left(\cosh^{-1}\left(\frac{2\Lambda}{k} - |\cos\nu|\right) - \cosh^{-1}\left(\frac{2\Lambda}{sk} + |\cos\nu|\right)\right) \tag{4.9}$$

Note that we must have $\left(\frac{2\Lambda}{k} + \cos(\nu)\right) > 1$ for $\cosh^{-1}$ to have real value. This is always satisfied whenever $k < \Lambda$. The ν integral is difficult to do analytically, so we will only look at the limit where $k \ll \Lambda$. This leads to

$$\frac{\alpha}{4} v_F \boldsymbol{\sigma}\cdot\boldsymbol{k}\left(\log s - \frac{(1+s)}{\pi}\frac{k}{\Lambda} + O\left((k/\Lambda)^2\right)\right) \tag{4.10}$$

where we have used $\alpha = \frac{e^2}{v_F}$

The above calculation shows a logarithmic correction to the Fermi velocity $v_F' = v_F(1 + \frac{\alpha}{4}\log(s))$. This is an experimentally verified[13] well known phenomenon.

4.2.2 Polarisation

Next we have the polarisation diagram, which gives the self energy of the auxilary Bosonic field. The diagram 4.3 translates to

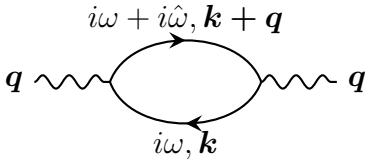

Figure 4.3: Polarisation Bubble diagram

$$\Pi(\hat{\omega}, \boldsymbol{q}) = \int_{-\infty}^{\infty} \frac{d\omega}{2\pi} \int \frac{d^2\boldsymbol{k}}{(2\pi)^2} G^{(0)}(i\omega, \boldsymbol{k}) G^{(0)}(i\omega + i\hat{\omega}, \boldsymbol{k}+\boldsymbol{q}) \tag{4.11}$$

with a trace over the sublattice indices. Doing the $\hat{\omega}$ integral we obtain

$$-2\int \frac{d^2\boldsymbol{k}}{(2\pi)^2} \frac{v_F(k + |\boldsymbol{k}+\boldsymbol{q}|)}{\hat{\omega}^2 + v_F^2(k+|\boldsymbol{k}+\boldsymbol{q}|)^2}\left[1 - \frac{\boldsymbol{k}.(\boldsymbol{k}+\boldsymbol{q})}{k|\boldsymbol{k}+\boldsymbol{q}|}\right] \tag{4.12}$$

Using the same substitution as earlier we get the equation

$$-\frac{v_F q^3}{4\pi^2}\int_0^{2\pi} d\nu \int_{\mu_{\min}}^{\mu_{\max}} d\mu \frac{\cosh(\mu)\sin^2(\nu)}{\hat{\omega}^2 + v_F^2 q^2 \cosh^2(\mu)} \tag{4.13}$$

The μ integral can be done analytically although like the previous case the ν integral can only be done if we take the limit $q \ll \Lambda$

$$
\begin{aligned}
&- \frac{v_F q^3}{4\pi^2} \int_0^{2\pi} d\nu \frac{\tan^{-1}\left(\frac{q v_F \sinh\mu}{\sqrt{q^2 v_F^2 + \hat{\omega}^2}}\right)}{q v_F \sqrt{q^2 v_F^2 + \hat{\omega}^2}} \Big|_{\mu=\mu_{\min}}^{\mu=\mu_{\max}} \\
&= - \frac{q^2}{4\pi^2 \sqrt{q^2 v_F^2 + \hat{\omega}^2}} \left(\pi \tan^{-1}\left(\frac{2 v_F \Lambda}{\hat{\omega}}\right) - \frac{q v_F \hat{\omega} \left(4 + 3\pi \tan^{-1}\left(\frac{2 v_F \Lambda}{s\hat{\omega}}\right)\right)}{3(4 v_F^2 \Lambda^2 + \hat{\omega}^2)} + O\left((q/\Lambda)^2\right) \right)
\end{aligned}
\tag{4.14}
$$

Having the polarisation function allows us to calculate the dielectric function $\epsilon(\hat{\omega}, q) = 1 + \frac{2\pi e^2}{q} \Pi(\hat{\omega}, q)$ which shows how the Coulomb gets dressed ($\frac{2\pi e^2}{q} \to \frac{2\pi e^2}{\epsilon(\hat{\omega}, q) q}$).

Chapter 5

Non perturbative calculations

5.1 Exact FRG equations

Functional Renormalisation Group flow equations capture the mode elimination in the Wilsonian Renormalisation Group framework exactly. To derive them we have to introduce a cutoff[1] Λ to our theory which will act as if the process of mode elimination has been done for momentum above the cutoff. The cutoff is introduced in the free part of the theory i.e. in the propagator of the free part $G_0 \to G_{0,\Lambda}$. We require the following to be satisfied in the deformed propagator.

$$G_{0,\Lambda} = \begin{cases} G_0 & \text{for } \Lambda \to 0 \\ 0 & \text{for } \Lambda \to \infty \end{cases} \tag{5.1}$$

This implies that we recover the original theory if we remove the cutoff and if the cutoff is large then the propagator is switched off (see [8]). There are many possible choices on how to introduce the cutoff. Here we will follow the most common choice of factoring out the cutoff dependence.

$$G_{0,\Lambda} = \Theta_\Lambda G_0 \tag{5.2}$$

This means that the multiplicative factor has to satisfy

$$\Theta_\Lambda = \begin{cases} 1 & \text{for } \Lambda \to 0 \\ 0 & \text{for } \Lambda \to \infty \end{cases} \tag{5.3}$$

[1]For easier notaion we will write Λ_0 as the highest cutoff typically determined by the lattice size($\approx \frac{\pi}{a}$) and Λ as the current cutoff as we keep reducing the cutoff.

Depending on the choice of this function various cutoff scheme has been developed. For example here we will work with momentum cutoff scheme where this function is only dependent on the momentum. Then we can say that $\Theta_\Lambda = \Theta(k-\Lambda)$. Where the previous restriction on the function means that the function vanishes for the argument being a large negative number and become unity for large positive number. So we can introduce a width of ϵ around 0 (momentum near cutoff) outside which the function essentially becomes either 0 or 1. This prompt us to work in a sharp momentum cutoff scheme where we take this width to be zero and get the familiar Heaviside Theta function.

$$\lim_{\epsilon\to 0}\Theta_\epsilon(k-\Lambda) = \theta(k-\Lambda) \tag{5.4}$$

We also introduce the derivative of this function as we are interested in the the differential equation of the generating funcitonal.

$$\delta_\epsilon(k-\Lambda) = -\frac{\partial}{\partial\Lambda}\Theta_\epsilon(k-\Lambda) \tag{5.5}$$

Note that this also goes to a Dirac delta function in the limit of sharp momentum cutoff.

As the cutoff Λ only enters in the propagator and the interaction part remains cutoff independent, we can calculate the derivative of each irreducible vertices with respect to the cutoff and obtain the differential equation known as the FRG equations. Here we will not derive them. The interested reader may look at reference [8]. We will only quote the exact FRG equations for spinless Fermions as given in [9].

Let $G_j(K)$ be the exact propagator of the Fermions and $V(Q)$ be the propagator of the auxiliary scalar field where j is the index labels the valley and K is short hand for $(i\omega, \boldsymbol{k})$. Finally, let $\Gamma_j(K,Q)$ be the exact Vertex where a Fermion of momentum K and a Boson of momentum Q come in and a Fermion of momentum $K+Q$ goes out. Then the exact FRG equations are

$$\partial_\Lambda\Sigma_j(K) = \int_Q V(Q)\dot{G}_j(K-Q)\Gamma_j(K-Q,Q)\Gamma_j(K,-Q) \tag{5.6a}$$

$$\partial_\Lambda\Pi(Q) = \sum_j\int_K [\dot{G}_j(K)G_j(K-Q) + \dot{G}_j(K-Q)G_j(K)]\Gamma_j(K,-Q)\Gamma_j(K-Q,Q) \tag{5.6b}$$

$$\begin{aligned}\partial_\Lambda\Gamma_j(K,Q) \;=\; & \int_{Q'} V(Q')[\dot{G}_j(K+Q-Q')G_j(K-Q') + \dot{G}_j(K-Q')G_j(K+Q-Q')] \\ & \times\Gamma_j(K+Q-Q',Q')\Gamma_j(K,-Q')\Gamma_j(K-Q',Q)\end{aligned} \tag{5.6c}$$

where we have used the notation $\dot{G}_\Lambda = -G_\Lambda\partial_\Lambda G_{0,\Lambda}^{-1}G_\Lambda$ which is called the single scale propagator. Also $V(Q) = \frac{2\pi e^2}{\epsilon_\Lambda(Q)q}$ where the dielectric function obtained from the

polarisation using $\epsilon_\Lambda(Q) = 1 + \frac{2\pi e^2}{q}\Pi(Q)$.

5.2 Numerical Solutions

The exact FRG equations quoted above are too complicated to solve. So we will try to make it more manageable by adding some more assumptions and gradually relax them as far as we can.

Firstly we will rederive the results in paper [9] by Kopietz et al.

We start with the expansion for the self energy for small ω and k

$$\Sigma_\Lambda(K) = V_\Lambda(k)\sigma.\mathbf{k} + (1 - Z_\Lambda^{-1})i\omega + O(\omega^2) \tag{5.7}$$

where, Z_Λ is the wave function renormalisation factor [2]. This would imply that our cutoff dependent propagator and the single scale propagator is given by

$$G_\Lambda(K) = -\theta(q-\Lambda)Z_\Lambda \frac{i\omega + v_\Lambda(k)\sigma.\mathbf{k}}{\omega^2 + v_\Lambda(k)^2k^2} \tag{5.8}$$

$$\dot{G}_\Lambda(K) = -\delta(q-\Lambda)Z_\Lambda \frac{i\omega + v_\Lambda(k)\sigma.\mathbf{k}}{\omega^2 + v_\Lambda(k)^2k^2} \tag{5.9}$$

where $v_\Lambda(k) = Z_\Lambda(v_F + V_\Lambda(k))$. Note that to derive the single scale propagator we used the Dyson equation $G^{-1} = G_0^{-1} - \Sigma$ and Morris Lemma [14] (see footnote). [3]

Next, we ignore the FRG equation for the vertex and take the zero external momentum limit for the vertex i.e. $i\Gamma_\Lambda(0,0) = i\gamma_\Lambda$. This reduces a lot of our calculations. We then get two coupled integro-differential equations to solve. There are two unknowns which we do not have control over, the wave-function renormalisation factor and the vertex function. Fortunately, due to a Ward identity these two are related and in the zero external momentum limit they satisfy $Z_\Lambda\gamma_\Lambda = 1$ [15]. This is a huge simplification which is essential for proceeding further with the equations. Moreover,

[2] The bare Hamiltonian $H_0 = \bar{\psi}G_0^{-1}\psi$ and the Renormalised Hamiltonian is $H_R = \bar{\psi}_R G^{-1}\psi_R$. Now using the facts that $G^{-1} = G_0^{-1} - \Sigma$ and $\psi = Z^{1/2}\psi_R$ we get the form above.

[3] Single scale propagator

$$\dot{G}_\Lambda(\boldsymbol{k}) = -\frac{\partial_\Lambda G_{0,\Lambda}(\boldsymbol{k})}{(1 - G_{0,\Lambda}(\boldsymbol{k})\Sigma_\Lambda(\boldsymbol{k}))^2} = -\frac{\delta(k-\Lambda)}{(i\omega - v_F\boldsymbol{\sigma}\cdot\boldsymbol{k})\left(1 - \frac{\theta(k-\Lambda)}{i\omega - v_F\boldsymbol{\sigma}\cdot\boldsymbol{k}}(V_\Lambda(k)\sigma.\mathbf{k} + (1-Z_\Lambda^{-1})i\omega)\right)^2}$$

To handle the theta function in the denominator we use the Morris Lemma [14]. $\delta(x)f(\theta(x)) = \delta(x)\int_0^1 dt f(t)$. This gives

$$\dot{G}_\Lambda(\boldsymbol{k}) = -\frac{\delta(k-\Lambda)}{(i\omega - v_F\boldsymbol{\sigma}\cdot\boldsymbol{k})\left(1 - \frac{1}{i\omega - v_F\boldsymbol{\sigma}\cdot\boldsymbol{k}}(V_\Lambda(k)\sigma.\mathbf{k} + (1-Z_\Lambda^{-1})i\omega)\right)}$$

Simplifying this gives the equation quoted in 5.8

following the work in [9] we will also assume that the polarisation function does not have a frequency dependence. Then the equation for the self energy becomes

$$\partial_\Lambda \Sigma(i\omega, \mathbf{k}) = -\gamma_\Lambda^2 Z_\Lambda \frac{e^2}{4\pi} \int_{-\infty}^{\infty} \frac{d\omega}{2\pi} \int d^2\mathbf{q} \frac{\delta(q-\Lambda)}{\epsilon_\Lambda(0, \mathbf{k}-\mathbf{q})|\mathbf{k}-\mathbf{q}|} \frac{i\omega + v_\Lambda(q)\sigma.\mathbf{q}}{\omega^2 + (v_\Lambda(q)q)^2} \tag{5.10}$$

This makes the ω integral trivial as we have a single pole at $\pm v_\Lambda(q)q$ for $i\omega$. Note that we need to manually put a damping factor to make the integrand vanish at infinity so that we can close the contour on one half of the complex plane in $i\omega$. We choose the right hand side hence only include the positive pole. This gives the following result

$$\partial_\Lambda \Sigma(k) = -\frac{e^2}{4\pi} \int d^2\mathbf{q} \frac{\delta(q-\Lambda)}{\epsilon_\Lambda(0, |\mathbf{k}-\mathbf{q}|)|\mathbf{k}-\mathbf{q}|} \frac{\sigma.\mathbf{q}}{q} \tag{5.11}$$

Note that, under this assumption Z_Λ becomes unity and does not renormalise (so is the case for the vertex function γ_Λ due to the Ward identity).

If we take $\mathbf{k} = k(1,0)$ and $\mathbf{q} = q(\cos(\phi), \sin(\phi))$ then

$$\begin{aligned} \Lambda\partial_\Lambda \Sigma(\boldsymbol{k}) &= -\frac{e^2}{4\pi}\sigma.\mathbf{k}\frac{\Lambda}{k}\int_0^{2\pi} d\phi \frac{\cos(\phi)}{\epsilon_\Lambda\left(0, \sqrt{k^2+\Lambda^2-2k\Lambda\cos(\phi)}\right)\sqrt{1-2(k/\Lambda)\cos(\phi)+(k/\Lambda)^2}} \\ \Lambda\partial_\Lambda v_\Lambda(k) &= -\frac{e^2}{4\pi}\frac{\Lambda}{k}\int_0^{2\pi} d\phi \frac{\cos(\phi)}{\epsilon_\Lambda\left(0, \sqrt{k^2+\Lambda^2-2k\Lambda\cos(\phi)}\right)\sqrt{1-2(k/\Lambda)\cos(\phi)+(k/\Lambda)^2}} \end{aligned} \tag{5.12}$$

Now for the polarisation function without the frequency dependence

$$\partial_\Lambda \Pi_\Lambda(q)_1 = -\int \frac{d^2\mathbf{k}}{(2\pi)^2} \frac{\delta(k-\Lambda)\theta(|\mathbf{k}+\mathbf{q}|-\Lambda)}{v_\Lambda(k)k + v_\Lambda(|\mathbf{k}+\mathbf{q}|)|\mathbf{k}+\mathbf{q}|} \left(1 - \frac{\mathbf{k}.(\mathbf{k}+\mathbf{q})}{k|\mathbf{k}+\mathbf{q}|}\right) \tag{5.13}$$

and a second term with $\mathbf{k}+\mathbf{q}$ and $\mathbf{k}$ interchanged. These two terms give the exact same contribution so we will consider just one term and multiply it with a factor of 2. To simplify the calculation we will go to elliptical co-ordinates and define $\mathbf{q} = q(1,0)$ and $\mathbf{k} = \frac{q}{2}(\cosh(\mu)\cos(\nu) - 1, \sinh(\mu)\sin(\nu))$. Substituting this into the previous equation gives the following equation

$$\begin{aligned} \partial_\Lambda \epsilon_\Lambda(q) = \frac{2\pi e^2}{q}\partial_\Lambda \Pi_\Lambda(q) = -\frac{2e^2}{\pi}\int_0^{\frac{\pi}{2}} d\nu \frac{\theta(\frac{2\Lambda}{q} + \cos\nu - 1)}{v_\Lambda(\Lambda)\Lambda + (\Lambda + q\cos(\nu))v_\Lambda(\Lambda + q\cos(\nu))} \\ \times \frac{q\sin^2(\nu)}{\sqrt{(2\Lambda + q\cos(\nu))^2 - q^2}} \end{aligned} \tag{5.14}$$

Note that the Heaviside theta function in 5.13 is already satisfied as $\cos\nu > 0$ in the integration limit. But we must have $\frac{2\Lambda}{q} + \cos\nu > 1$ to ensure $\cosh^{-1}$ have real values. This is encoded in another Heaviside theta function.

The two coupled differential equations for v_Λ and ϵ_Λ eqs 5.12 and 5.14, can be solved numerically and the results are given in the next section.

5.2.1 Calculation Details

The equations in the last section can be numerically solved [4]. Firstly, note that these differential equations are not coupled to each other in the momentum variable. So they are coupled ordinary differential equations rather than partial differential equations. The boundary condition for the system of ODE is that the dielectric function and Fermi velocity at the highest cutoff goes to unity and v_F respectively. So then we need to start from the highest cutoff and then using the equations we update the values at the next cutoff and so on till we reach zero cutoff. To achieve the algorithm stated above we first create a $m \times n$ grid to represent the discretised version of momentum and cutoff. Each site in the grid carries a momentum and a cutoff. For simplicity we will take the highest cutoff as 1 or equivalently work with the variable k/Λ_0 and Λ/Λ_0. This makes the grid running from 0 to 1. Now we know the values at $\Lambda = \Lambda_0$ $v_\Lambda(k) = v_F$ and $\epsilon_\Lambda(0, q) = 1$. Or in the descretized language for $\Lambda^{(n)} = 1$ $v(i, n) = 1 \forall 0 < i \leq m$ and $\epsilon(i, n) = 1 \forall 0 < i \leq m$. From the equations 5.12 and 5.14 we then can calculate the changes in velocity and dielectric function after doing a numerical integration over the angular co-ordinate. This is straight-forward and only thing to remember is the implementation of θ function. Once getting the δv and $\delta\epsilon$ for each momentum we can get the velocity and dielectric function at the next cutoff. $v(i, n-1) = v(i, n) + \delta v_i$ and $\epsilon(i, n-1) = \epsilon(i, n) + \delta\epsilon_i$. Continuing the process we will be able to get till zero cutoff.

5.2.2 Results

Below in the figure 5.1 the velocity and dielectric function at different momentum as we do the renormalisation procedure.

The physically relevant information is when we have completed the renormalisation process i.e. $\Lambda = 0$. The values of velocity and dielectric function at that limit is shown in the figure 5.2. The renormalised velocity shows the familiar logarithmic behavior. A curve fitting tells the velocity follows $a + b\log(k/\Lambda_0)$ with $a = 1.39$ and $b = -0.57$ in the unit of Fermi Velocity. The result matches with the one loop calculation where we have the coefficient of logarithm $-\frac{\alpha}{4} \approx -0.55$. The polarisation function significantly differ from the Random Phase Approximation (RPA) [16] result $\epsilon_{\text{RPA}}(q) = 1 + \pi\alpha/4 \approx 1.73$ however if we take the limit $\Lambda_0 \to \infty$ in eqn 5.14 we recover this result.

[4] The codes can be found at https://github.com/biplab37/Code_Thesis

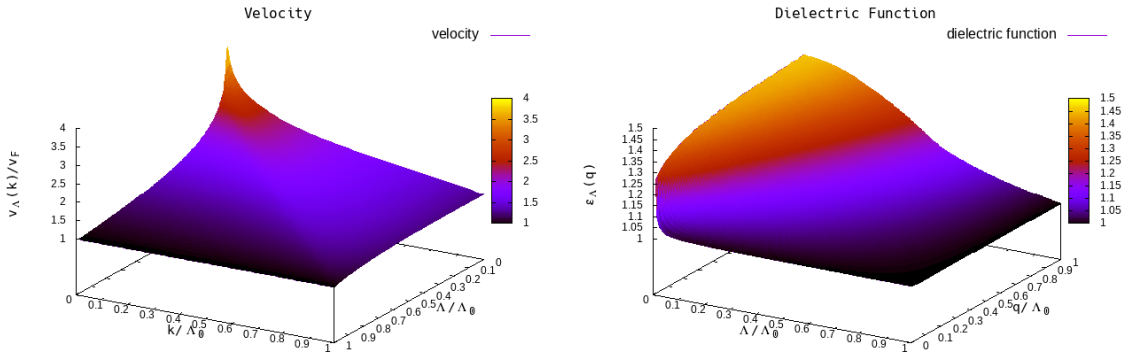

(a) Velocity *(b) Dielectric Function*

Figure 5.1: Surface Plot of velocity and dielectric function as functions of cutoff and momentum

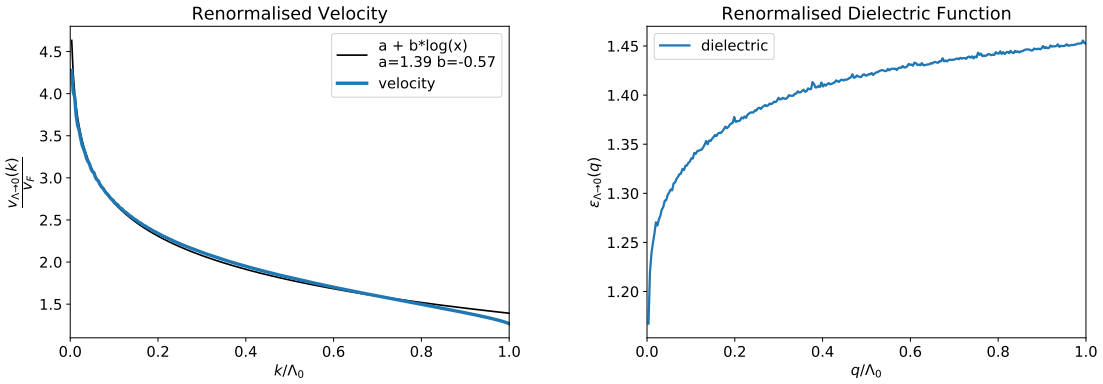

(a) Renormalised Velocity *(b) Renormalised Dielectric Function*

Figure 5.2: Renormalised Velocity and Dielectric function.

5.2.3 Bosonic Momenta inside Shell

In the above calculation as well as the theory that is developed by Kopietz, in the momentum cutoff scheme only the Fermionic momenta are taken inside the shell ($\frac{\Lambda}{s} < k < \Lambda$) as the cutoff was only introduced for the Fermionic propagator. While we should have required all the momentum that are integrated out to lie inside the shell. This also means that we must have the bosonic momenta in the self energy calculation inside the integrated out shell. This will modify our equations a little bit. Equation 5.6a gets modified to

$$\partial_\Lambda \Sigma_j(K) = \int_Q [V(Q)\dot{G}_j(K-Q) + \dot{V}(Q)G(K-Q)]\Gamma_j(K-Q,Q)\Gamma_j(K,-Q) \quad (5.15)$$

where we have to introduce a Heaviside theta function in the definition of the Bosonic propagator $V(Q)$ and define the single scale propagator for the Boson as

$$V(Q) = \theta(q-\Lambda)\frac{2\pi e^2}{q + 2\pi e^2 \Pi(Q)}$$
$$\dot{V}(Q) = \delta(q-\Lambda)\frac{2\pi e^2}{q + 2\pi e^2 \Pi(Q)} \tag{5.16}$$

The equation 5.15 is similar to the FRG equation for the polarisation 5.6b so we will use the same elliptical cooridates substitution. Unlike the polarisation case two terms in this equation is not equal and we are left with the FRG equation for the self energy $\partial_\Lambda \Sigma(K)$ as

$$-\frac{e^2}{2\pi}\boldsymbol{\sigma}\cdot\mathbf{k}\int_0^{\pi/2} d\nu \frac{\theta(\frac{2\Lambda}{k}+\cos\nu-1)}{\sqrt{(2\Lambda+k\cos(\nu))^2-k^2}}\left(\frac{(\frac{2\Lambda}{k}+\cos(\nu))\cos(\nu)-1}{\epsilon_\Lambda(\Lambda+k\cos(\nu))} - \frac{(\frac{2\Lambda}{k}+\cos(\nu))\cos(\nu)+1}{\epsilon_\Lambda(\Lambda)}\right)$$

Solving this equation along with the polarisation given in eqn 5.14 the results are shown in fig 5.3, together with the same fitting function as used earlier. Note that the coefficients of the fit that we obtain are silghtly different from what we got earlier. The polarisation function saturates much faster in this case.

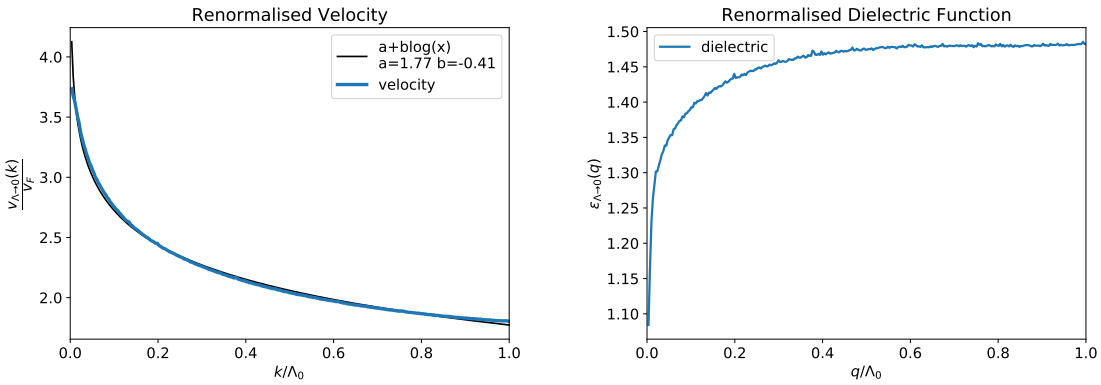

(a) Renormalised Velocity *(b) Renormalised Dielectric Function*

Figure 5.3: Renormalised Velocity and Dielectric Function with both momentum inside shell

Chapter 6

Finite Temperature Calculations

In this chapter, we extend the results in the last chapter to finite temperature using Matsubara Formalism. Frequency integral from $-\infty$ to ∞ is replaced by sum over the Matsubara frequencies $\omega_n = 2n\frac{\pi}{\beta}$ for bosons and $\hat{\omega}_n = (2n+1)\frac{\pi}{\beta}$ for fermions. See the excellent textbook by Mahan [17] for a detailed introduction to finite temperature calculations.

6.1 Self Energy

Using the Matsubara frequencies the FRG equation for the self energy at temperature $T = \frac{1}{k_B\beta}$can be rewritten as

$$\partial_\Lambda \Sigma(\boldsymbol{k}) = -\frac{e^2}{2\pi}\frac{1}{\beta}\int_{\mathbf{q}}\sum_{n=-\infty}^{\infty}\frac{\theta(q-\Lambda)\theta(|\mathbf{k}+\mathbf{q}|-\Lambda)}{|\mathbf{k}+\mathbf{q}|\epsilon_\Lambda(|\mathbf{k}+\mathbf{q}|)}\frac{i\hat{\omega}_n + v_\Lambda(q)\boldsymbol{\sigma}\cdot\mathbf{q}}{(i\hat{\omega}_n)^2 - (v_\Lambda(q)q)^2} \tag{6.1}$$

where frequency independence of the dielectric function is assumed as in last chapter. Then the Matsubara sum is simple.

First, note that the functions[1] $f_\eta(z) = \frac{1}{e^{\eta\beta z}-\eta}$ have poles at the Matsubara frequencies with $\eta = +1$ for bosons and $\eta = -1$ for fermions. If then we take a function $F(z)$ which is obtained by substituting z in place of $i\hat{\omega}_n$ in eqn 6.1 without the $-1/\beta$ factor then for a contour as shown in the figure 6.1 the integral $\int_{\mathcal{C}} f_{-1}(z)F(z)dz$ evaluates to zero as we take the radius to infinity. Poles are shown in the figure 6.1. For

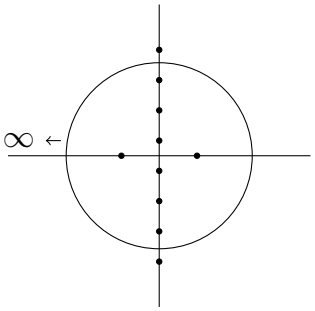

Figure 6.1: self energy contour

[1]same result is obtained if we use slightly different functions $f_\eta(z) = \frac{1}{e^{-\eta\beta z}-\eta}$

the poles on the vertical axis we recover the sum in eqn 6.1 as the residue of $f_{-1}(z)$ is $-\frac{1}{\beta}$. So as the integral over the contour vanishes, the contribution from the other two poles must be equal and opposite to the Matsubara sum in 6.1. Therefore the RHS of the FRG equation for the self energy becomes

$$-\frac{e^2}{4\pi}\int_{\mathbf{q}}\frac{\theta(q-\Lambda)\theta(|\mathbf{k}+\mathbf{q}|-\Lambda)}{|\mathbf{k}+\mathbf{q}|\epsilon_\Lambda(|\mathbf{k}+\mathbf{q}|)}\left(\frac{1}{e^{-\beta v_\Lambda(q)q}+1}\left(1+\frac{\boldsymbol{\sigma}\cdot\mathbf{q}}{q}\right)+\frac{1}{e^{\beta v_\Lambda(q)q}+1}\left(1-\frac{\boldsymbol{\sigma}\cdot\mathbf{q}}{q}\right)\right) \tag{6.2}$$

We can ignore the Identity part and focus on the part proportional to sigma matrices as the identity part will generate chemical potential like terms which can be removed by adding counterterm. The part with sigma

$$\frac{e^2}{4\pi}\int_{\mathbf{q}}\frac{\theta(q-\Lambda)\theta(|\mathbf{k}+\mathbf{q}|-\Lambda)}{|\mathbf{k}+\mathbf{q}|\epsilon_\Lambda(|\mathbf{k}+\mathbf{q}|)}\frac{\boldsymbol{\sigma}\cdot\mathbf{q}}{q}\tanh(\frac{\beta v_\Lambda(q)q}{2}) \tag{6.3}$$

Hence the differential equation

$$\partial_\Lambda\Sigma(k)=\frac{e^2}{2\pi}\int_{\mathbf{q}}\frac{\delta(q-\Lambda)\theta(|\mathbf{k}+\mathbf{q}|-\Lambda)+\theta(q-\Lambda)\delta(|\mathbf{k}+\mathbf{q}|-\Lambda)}{|\mathbf{k}+\mathbf{q}|\epsilon_\Lambda(|\mathbf{k}+\mathbf{q}|)}\frac{\boldsymbol{\sigma}\cdot\mathbf{q}}{q}\tanh(\frac{\beta v_\Lambda(q)q}{2}) \tag{6.4}$$

with the usual elliptic coordinate substitution we get

$$\begin{aligned}\partial_\Lambda v_\Lambda(k)=\frac{e^2}{2\pi}\int_0^{\pi/2}d\nu\,&\frac{\theta(\frac{2\Lambda}{k}-\cos\nu-1)}{\sqrt{(2\Lambda+k\cos(\nu))^2-k^2}}\Big(\frac{(\frac{2\Lambda}{k}+\cos(\nu))\cos(\nu)-1}{\epsilon_\Lambda(\Lambda+k\cos(\nu))}\tanh(\frac{\beta v_\Lambda(\Lambda)\Lambda}{2})\\&-\frac{(\frac{2\Lambda}{k}+\cos(\nu))\cos(\nu)+1}{\epsilon_\Lambda(\Lambda)}\tanh(\frac{\beta v_\Lambda(\Lambda+k\cos(\nu))(\Lambda+k\cos(\nu))}{2})\Big)\end{aligned} \tag{6.5}$$

6.2 Polarisation Function

The polarisation function in finite temperature setting

$$\Pi_\Lambda(i\omega_n,q)=\frac{1}{\beta}\int_{\mathbf{k}}\sum_{m\in\mathbb{Z}}\frac{i\hat{\omega}_m+\sigma.\mathbf{k}}{(i\hat{\omega}_m)^2-(v_\Lambda(k)k)^2}\frac{i(\omega_n+\hat{\omega}_m)+\boldsymbol{\sigma}\cdot(\mathbf{k}+\mathbf{q})}{(i\omega_n+i\hat{\omega}_m)^2-(v_\Lambda(|\mathbf{k}+\mathbf{q}|)|\mathbf{k}+\mathbf{q}|)^2} \tag{6.6}$$

Same trick used in the evaluation of finite temperature self energy can be used here as well. The four poles are at $\pm kv_\Lambda(k)$ and $-i\omega_n\pm v_\Lambda(|\mathbf{k}+\mathbf{q}|)|\mathbf{k}+\mathbf{q}|$. Before quoting the result lets define $k_1=\Lambda$ and $k_2=\Lambda+q\cos(\nu)$ along with $v_1=v_\Lambda(k_1)$ and $v_2=v_\Lambda(k_2)$ for convenience. Then without the frequency dependence $\partial_\Lambda\epsilon_\Lambda(q)=\frac{2\pi e^2}{q}\partial_\Lambda\Pi_\Lambda(0,q)$ is given by

$$-\frac{2e^2}{\pi q}\int_0^{\pi/2}\frac{k_2(2v_1k_1^2+v_2(k_1^2+k_2^2-q^2))\tanh(\frac{\beta v_1k_1}{2})-k_1(2v_2k_2^2+v_1(k_1^2+k_2^2-q^2))\tanh(\frac{\beta v_2k_2}{2})}{\sqrt{(k_1+k_2)^2-q^2(v_1^2k_1^2-v_2^2k_2^2)}} \tag{6.7}$$

The equation have a singular 0/0 form where $k_1v_1 \approx k_2v_2$. For numerical stability we will approximate the equation where $k_1v_1 \approx k_2v_2$. But first define $\tanh(\frac{\beta v_1 k_1}{2}) = t_1$ and $\tanh(\frac{\beta v_2 k_2}{2}) = t_2$ to rewrite the above equation in a compact form.

$$-\frac{2e^2}{\pi q}\left(\sqrt{(k_1+k_2)^2-q^2}\frac{k_2v_2t_1-k_1v_1t_2}{k_1^2v_1^2-k_2^2v_2^2}+\frac{2k_1k_2(t_1+t_2)}{\sqrt{(k_1+k_2)^2-q^2}(k_1v_1+k_2v_2)}\right) \tag{6.8}$$

Near the points where $k_1v_1 \approx k_2v_2$, t_1 becomes very close to t_2 and in the first term $k_d1v_1 - k_2v_2$ can be factored out from the numerator and denominator which leaves

$$-\frac{2e^2}{\pi q}\left(-\frac{t_1\sqrt{(k_1+k_2)^2-q^2}}{k_1v_1+k_2v_2}+\frac{2k_1k_2(t_1+t_2)}{\sqrt{(k_1+k_2)^2-q^2}(k_1v_1+k_2v_2)}\right) \tag{6.9}$$

6.3 Numerical Results

The equations 6.4 and 6.8 can be solved numerically by the same method used earlier for each temperature separately. We calculate the renormalised velocity and dielectric function at different temperatures. The figure 6.2 and 6.3 shows the variation of velocity and dielectric with temperature. We have used unit less temperature variable $t = \frac{k_BT}{\Lambda_0 v_F}$, where T is the absolute temperature and k_B is the Boltzmann constant.

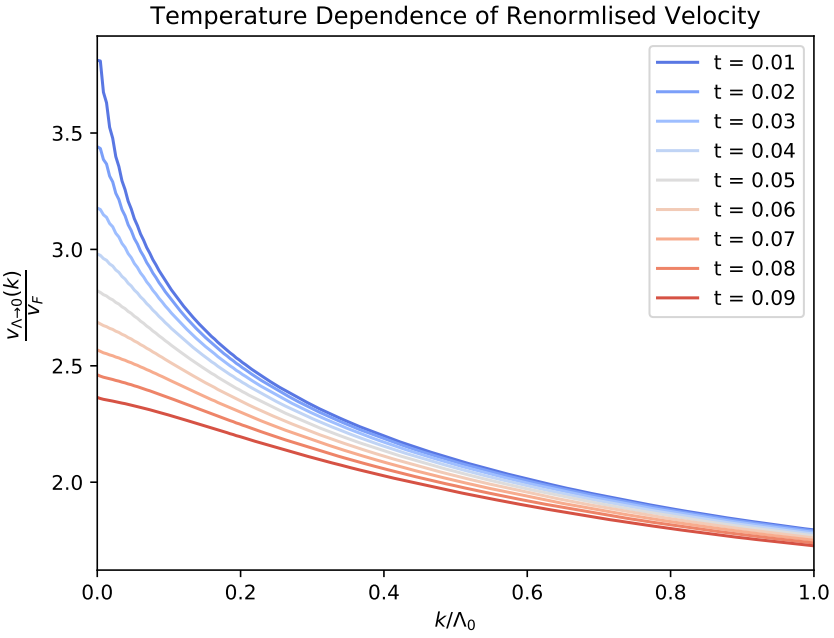

Figure 6.2: Temperature Dependence of Renormalised Velocity. $t = \frac{k_BT}{\Lambda_0 v_F}$

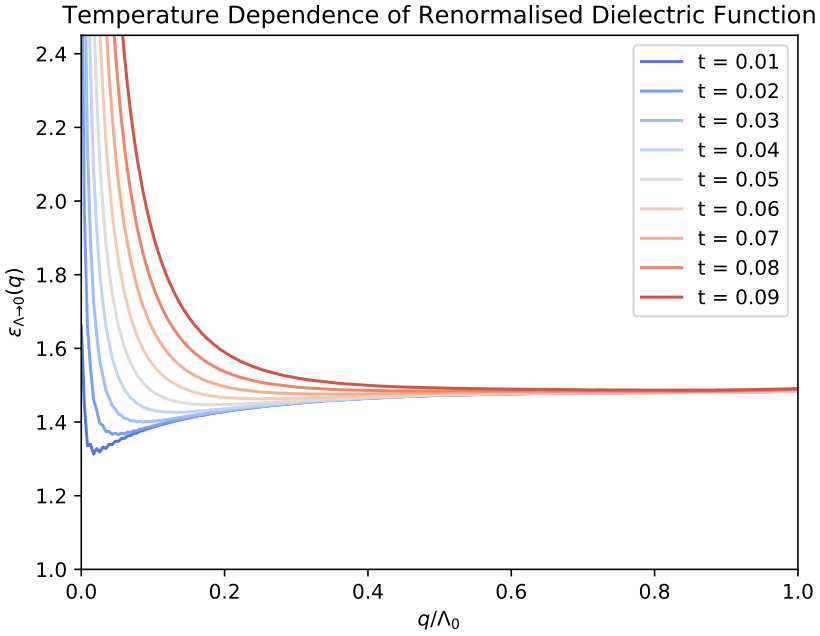

Figure 6.3: Temperature Dependence of Renormalised Dielectric Function. $t = \frac{k_B T}{\Lambda_0 v_F}$

As can be seen from the graph the velocity loses its logarithmic divergence at non zero temperature. While the dielectric function picks up divergence at small momentum. In both the graphs, we see variation from the zero temperature case only in the lower momenta. This is expected as the thermal energy which is roughly $k_B T$ should effect the states which are of similar energy scale. Energy dispersion without interaction is given by $v_F k$. Assuming roughly similar energy with the interaction, we can see that we expect momentum lower than $\frac{k}{\Lambda_0} \approx \frac{k_B T}{v_F \Lambda_0} = t$ to be effected. the graphs shows the expected behaviour.

Next, we try to quantify the behaviour of velocity and dielectric function at finite temperature. First, consider the equation for derivative of the dielectric function at zero temperature in 5.14. If we take the limit $q \to 0$ we get

$$\partial_\Lambda \epsilon_\Lambda(q \to 0) \approx -\frac{2e^2}{\pi} \int_0^{\pi/2} d\nu \frac{q \sin^2(\nu)}{4\Lambda^2 v_\Lambda(\Lambda)} = -\frac{\alpha q}{8\Lambda^2 v_\Lambda(\Lambda)/v_F} \tag{6.10}$$

For a fixed finite temperature same limit gives

$$\partial_\Lambda \epsilon_\Lambda(q \to 0) = \frac{\alpha}{q} \frac{1 - \tanh(\frac{\beta v_\Lambda(\Lambda)\Lambda}{2})}{v_\Lambda(\Lambda)/v_F} \tag{6.11}$$

The last two equations captures the results in the figure 6.3 as we can see a $\frac{1}{q}$ type divergence at finite temperature and linear behaviour at zero temperature for small

momenta.

For the velocity, consider the equation 6.4 in the $k \to 0$ limit

$$\partial_\Lambda(v_\Lambda(k \to 0)) = -\alpha \frac{v_F \beta \Lambda (v_\Lambda(\Lambda) + \Lambda v_\Lambda'(\Lambda)) + 2\sinh(\beta \Lambda v_\Lambda(\Lambda))}{8\Lambda \epsilon_\Lambda(\Lambda)(1 + \cosh(\beta \Lambda v_\Lambda(\Lambda)))} \tag{6.12}$$

In the temperature close to zero we can approximate a little further. Using the fact $2(1 + \cosh(x)) = 2 + e^x + e^{-x} \approx e^x$ and $2\sinh(x) = e^x - e^{-x} \approx e^x$ for large x.

$$\partial_\Lambda(v_\Lambda(k \to 0)/v_F) = -\frac{\alpha}{4\Lambda \epsilon_\Lambda(\Lambda)} - \frac{1}{\epsilon_\Lambda(\Lambda)} \alpha \beta (v_\Lambda(\Lambda) + \Lambda v_\Lambda'(\Lambda)) e^{-\beta \Lambda v_\Lambda(\Lambda)} \tag{6.13}$$

If we assume $\epsilon_\Lambda(\Lambda) \approx 1$ then the cutoff integral can be done and we have

$$v_\Lambda(k \to 0)/v_F = 1 - \frac{\alpha}{4} \log(\Lambda) + \alpha e^{-\beta \Lambda v_\Lambda(\Lambda)} - \alpha e^{-\beta \Lambda_0 v_F} \tag{6.14}$$

Note the logarithmic divergence in the velocity. At finite temperature, due to $\frac{1}{q}$ like divergence in the dielectric function this logarithmic divergence goes away.

Chapter 7

Pole Approximation

In the last two chapters we solved the coupled integro-differential with the assumption that the dielectric function does not have frequency dependence. In this chapter we will try to relax this condition. Retaining the frequency dependence was complicated as the frequency integral in the self energy has to be done analytically. Keeping track of all the poles and branch cuts that are arising in the dielectric function is very difficult numerically. Instead, we will try to model the frequency dependence in the polarisation with simple functions. The ideas in this chapter draws inspiration from [10]. In this paper, the authors have used the plasmon pole approximation (PPA) which models the inverse of the dielectric function with functions having simple poles. This method (PPA) is typically used along with frequency sum rule and the Krammers-Kronig relation to find the location of the pole and the residue at the pole. But as shown in the paper Graphene does not admit a proper f-sum rule, which leaves one free parameter to be fixed. So they took three different models of the pole and used the exact RPA result of the polarisation ([16]) to numerically determine the self energy. Their work was in the framework of perturbative RG, so it would be nice to do a similar calculation in the framework of functional renormalization group i.e. in a non-perturbative setting.

7.1 The Models

The idea of modeling the dielectric function with just a single pole is very promising as it simplifies a lot of complicated calculations. But the models that were used in ref [10] are not suitable for our case as we are working near the Dirac points and the plasmon frequency vanishes at those points. So the methods used in that paper are not very useful in our case. Instead we will take a different route as described below.

First, note that we are interested in doing the frequency integral in the self energy

term.

$$\partial_\Lambda \Sigma(i\omega, \mathbf{k}) = -\frac{e^2}{4\pi}\int_{-\infty}^{\infty}\frac{d\omega}{2\pi}\int d^2\mathbf{q}\frac{\delta(q-\Lambda)}{\epsilon_\Lambda(\bar{\omega},\mathbf{q})q}\frac{i(\omega+\bar{\omega})+v_\Lambda(q)\sigma.\mathbf{q}}{(\omega+\bar{\omega})^2+(v_\Lambda(q)q)^2} \tag{7.1}$$

We need to model the term $\frac{1}{\epsilon_\Lambda(\bar{\omega},\boldsymbol{q})}$, the inverse of dielectric function. Here we introduce two models with simple pole.

- **simple pole:** In this model we assume the simplest function with a simple pole.

$$\frac{1}{\epsilon_\Lambda(\omega,q)} = \frac{A_\Lambda(q)}{\omega^2-\omega_\Lambda(q)^2} \tag{7.2}$$

- **pole correction:** We separate the dominant contribution of unity to the dielectric function and add a function with simple pole as a correction to it. The paper [10] used model similar to this.

$$\frac{1}{\epsilon_\Lambda(\omega,q)} = 1 + \frac{A_\Lambda(q)}{\omega^2-\omega_\Lambda(q)^2} \tag{7.3}$$

7.2 Numerical Solution

The models introduced above has two free parameters, the location of the pole $\omega_\Lambda(q)$ and the residue $A_\Lambda(q)$ at the pole. To determine them, first note the polarisation function that we have

$$\Pi_\Lambda(Q) = -\int\frac{d^2\mathbf{k}}{(2\pi)^2}\theta(q-\Lambda)\theta(|\mathbf{k}+\mathbf{q}|-\Lambda)\frac{\xi_\Lambda(k)+\xi_\Lambda(|\mathbf{k}+\mathbf{q}|)}{(\xi_\Lambda(k)+\xi_\Lambda(|\mathbf{k}+\mathbf{q}|))^2+\hat{\omega}^2}\left(1-\frac{\mathbf{k}.(\mathbf{k}+\mathbf{q})}{k|\mathbf{k}+\mathbf{q}|}\right) \tag{7.4}$$

From this we can expand in small frequency ω to get corrections to dielectric functions

$$\epsilon_\Lambda(q,\omega) = X_\Lambda(q) + \omega^2 Y_\Lambda(q) + O(\omega^4) \tag{7.5}$$

where

$$\begin{aligned}\partial_\Lambda X_\Lambda(q) &= -\frac{2e^2}{\pi}\int_0^{\frac{\pi}{2}} d\nu \frac{\theta(\frac{2\Lambda}{q}-\cos\nu-1)}{v_\Lambda(\Lambda)\Lambda+(\Lambda+q\cos(\nu))v_\Lambda(\Lambda+q\cos(\nu))}\frac{q\sin^2(\nu)}{\sqrt{(2\Lambda+q\cos(\nu))^2-q^2}}\\ \partial_\Lambda Y_\Lambda(q) &= \frac{2e^2}{\pi}\int_0^{\frac{\pi}{2}} d\nu \frac{\theta(\frac{2\Lambda}{q}-\cos\nu-1)}{(v_\Lambda(\Lambda)\Lambda+(\Lambda+q\cos(\nu))v_\Lambda(\Lambda+q\cos(\nu)))^3}\frac{q\sin^2(\nu)}{\sqrt{(2\Lambda+q\cos(\nu))^2-q^2}}\end{aligned} \tag{7.6}$$

along with the boundary condition that $X_{\Lambda_0}(q) = 1$ and $Y_{\Lambda_0} = 0$

Before using $X_\Lambda(q)$ and $Y_\Lambda(q)$ to determine the $A_\Lambda(q)$ and $\omega_\Lambda(q)$, note that we are working in the imaginary time formulation. So, the frequencies in the models and frequencies in the 7.4 should not be compared directly. They are related by analytical continuation in the complex plane of frequency. Hence we will first analytically

continue the real frequencies in the models by substituting $\omega \to i\omega$ and then compare.

- For the first model we can simply use the following with the identification that $A_\Lambda(q) = \frac{1}{Y_\Lambda(q)}$ and $\omega_\Lambda(q)^2 = \frac{X_\Lambda(q)}{Y_\Lambda(q)}$

$$\frac{1}{\epsilon_\Lambda(\omega, q)} = \frac{1}{X_\Lambda(q) + \omega^2 Y_\Lambda(q)} \tag{7.7}$$

- For the second case we equate the two equations

$$1 - \frac{A_\Lambda(q)}{\omega^2 + \omega_\Lambda(q)^2} = \frac{1}{X_\Lambda(q) + \omega^2 Y_\Lambda(q)} \tag{7.8}$$

  Comparing these equations in small frequency limit we obtain

$$A_\Lambda(q) = -\frac{(X_\Lambda(q) - 1)^2}{Y_\Lambda(q)} \quad \omega_\Lambda^2(q) = -\frac{X_\Lambda(q)(X_\Lambda(q) - 1)}{Y_\Lambda(q)} \tag{7.9}$$

As $X_\Lambda(q)$ and $Y_\Lambda(q)$ can be easily computed numerically so we can get the pole and the residue at the pole easily. Now if we use this dielectric function instead of the frequency independent dielectric function then the self energy can be calculated.

Firstly we do the frequency integral in the self energy analytically. Then we are left with an equation similar to the equation we were dealing with earlier which can be numerically solved to get $\Sigma(\boldsymbol{k}, \omega)$, both its real and imaginary parts. But here we expand this for small frequencies and compare the equation with

$$\Sigma_\Lambda(\boldsymbol{k}, \omega) = \boldsymbol{\sigma}.\boldsymbol{k} V_\Lambda(k) + (1 - Z_\Lambda^{-1}) i\omega + O(\omega^2) \tag{7.10}$$

This helps us to calculate the wave function renormalisation factor $Z_\Lambda(k)$ and the renormalised velocity $v(k) = \lim_{\Lambda \to 0} Z_\Lambda(v_F + V_\Lambda(k))$.

The results are shown below in the figures 7.1 and 7.2 As can be seen from the figures pole correction model gives result closer to the result without the frequency dependence.

The wavefunction renormalisation factors for the models look widely different from each other. Although they have some similarities. For example, we are calculating the $Z_\Lambda(k)$ from the coefficient of $i\omega$ in eqn 7.10. This coefficient in both cases increases from a value close to zero as we go from higher to lower momentum. The singular behaviour in the pole correction $Z_\Lambda(k)$ comes when the coefficient crosses 1.

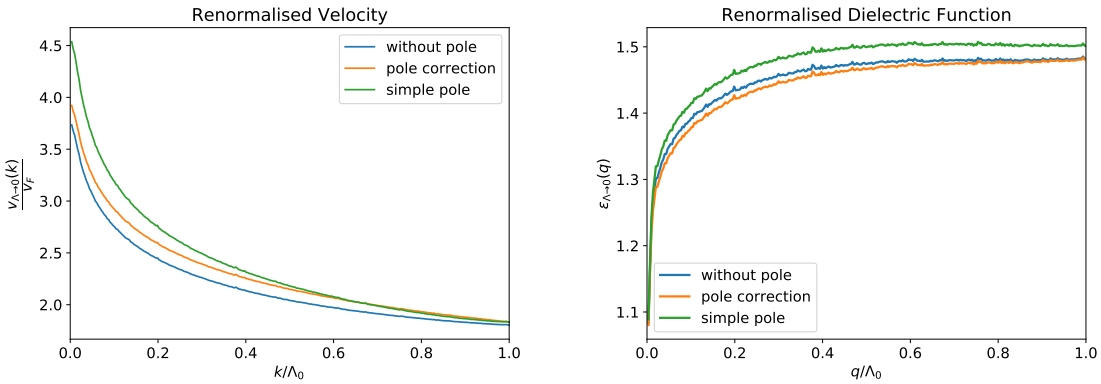

Figure 7.1: Renormalised velocity and dielectric function with different models of dielectric function

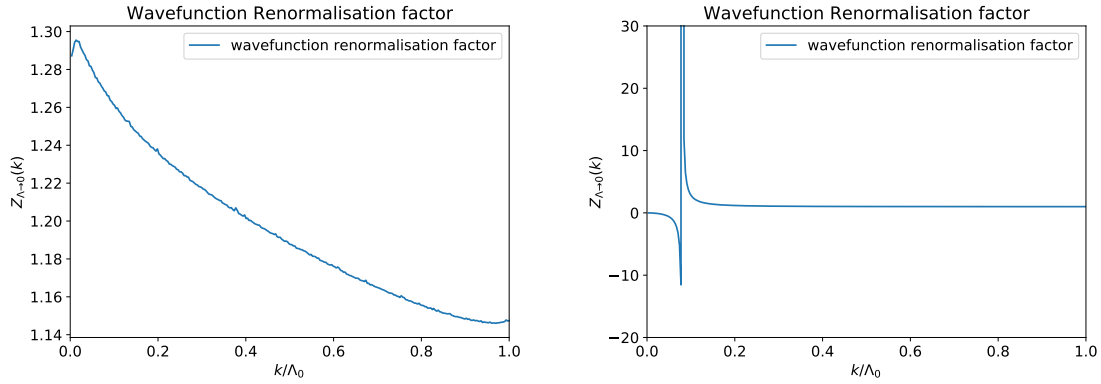

(a) simple pole *(b) pole correction*

Figure 7.2: Wave function renormalisation factor for the two models

7.3 Future Work

The work above can be extended in various ways. Some directions are

- In chapter 4, we saw that the first order correction to the polarisation function has a square root branch cut. Naturally, we should look for a model with square root branch cut

$$\frac{1}{\epsilon_\Lambda(q)} = 1 + \frac{A_\Lambda(q)}{\sqrt{\omega^2 - \omega_\Lambda(q)^2}} \tag{7.11}$$

  Similar numerical methods will work for this case as well.

- One can numerically evaluate both the real and imaginary part of the self energy as functions of both momentum and frequency. This will allow calculation of the Spectral function $A(\omega, k)$ which contain dynamical information of the system.

$$A(\omega, k) = \frac{2\ \mathrm{Im}\Sigma(\omega, k)}{(\omega - \mathcal{E}(k) - \mathrm{Re}\Sigma(\omega, k))^2 + (\mathrm{Im}\Sigma(\omega, k))^2} \tag{7.12}$$

Appendix A

Grassmann Algebra

Coherent States

For simplicity we ignore the spins i.e. we only consider spinless fermions. To calculate the partition function or any expectation values we need to take trace over states. For that we need to choose a suitable basis which simplifies our calculations. Fermionic coherent states are best suited as basis elements. Going with the notation used in the text let Ψ and $\Psi^\dagger$ be the annihilation and creation operator for Fermions. Then coherent states are the eigenstates of the annihilation operators.

$$\Psi|\psi\rangle = \psi|\psi\rangle \tag{A.1}$$

where ψ is the eigenvalue. Note that the anticommutativity of the operator forces anticommutativity in the eigenvalues as well.

$$\Psi_1\Psi_2|\psi_1,\psi_2\rangle = -\Psi_2\Psi_1|\psi_1,\psi_2\rangle \implies \{\psi_1,\psi_2\} = 0 \tag{A.2}$$

These relation are a reminder that the eigenvalues are not at all like the real or complex numbers that we are so familiar with. These new numbers are called Grassmann number honoring the inventor of the algebra of these numbers. Then in a similar manner we can write

$$\langle\bar{\psi}|\Psi^\dagger = \langle\bar{\psi}|\bar{\psi} \tag{A.3}$$

Finally, note that the anticommutativity property of the Grassmann numbers allow us to write the above coherent states as

$$|\psi\rangle = (1 - \psi\Psi^\dagger)|\Omega\rangle \tag{A.4}$$

$$\langle\bar{\psi}| = \langle\Omega|(1 - \Psi\bar{\psi}) \tag{A.5}$$

Action of Ψ on the first equation and using the anticommutativity of operators and the fact that $\psi^2 = 0$ we get back A.1. Similarly the second equation. One thing to be noted that $|\psi\rangle$ and $\langle\bar{\psi}|$ are not adjoint of each other as ψ and $\bar{\psi}$ are not related.

Properties of Coherent States and Grassmann Variables

First note the inner product of two states.

$$\begin{aligned}\langle\bar{\psi}|\psi\rangle &= \langle\Omega|(1-\Psi\bar{\psi})(1-\psi\Psi^\dagger)|\Omega\rangle \\ &= \langle\Omega|1-\psi\Psi^\dagger-\bar{\psi}\Psi+\bar{\psi}\psi\Psi\Psi^\dagger|\Omega\rangle \\ &= 1+\bar{\psi}\psi = e^{\bar{\psi}\psi}\end{aligned} \tag{A.6}$$

Next we would like to define integrals over Grassmann numbers. Due to the anticommutation relation square or higher power of a Grassmann number vanishes. So the most general function of Grassmann numbers are linear in them $f(\psi) = a + b\psi \;\; a, b \in \mathbb{C}$. So we just have to define the integral of 1 and ψ with respect to ψ. Requiring the relation $\int f(\psi+\eta)d\psi = \int f(\psi)d\psi$ for some η Grassmann number, to be satisfied, implies $\int d\psi = 0$. Then the linearity over the complex field puts the restriction that the $\int \psi d\psi$ to be some complex number. For convinience we will define it to be unity.

$$\int d\psi = 0 \quad \int \psi d\psi = 1 \tag{A.7}$$

One should remember that the differential element $d\psi$ is also a Grassmann number hence the relative position is important. These two definitions allows us to evaluate all the integrals that is needed. For example,

$$\int \bar{\psi}\psi d\psi d\bar{\psi} = 1 \tag{A.8}$$

$$\int e^{-a\bar{\psi}\psi} d\bar{\psi} d\psi = a \tag{A.9}$$

These two equations can be easily checked by calculations comprising couple of lines. The last equation can be generalised easily (just like the Gaussian integration)

$$\int e^{-\bar{\psi}M\psi}[d\bar{\psi}d\psi] = \det M \tag{A.10}$$

where we have abused the notation a little bit and assumed ψ's to be a d-vector with Grassmann entries and M being a diagonalisable $d \times d$ matrix over Complex numbers.

Similarly we have two more important result the resolution of identity and the trace formula.

$$I = \int |\psi\rangle\langle\bar{\psi}|e^{-\bar{\psi}\psi}d\bar{\psi}d\psi \tag{A.11}$$

$$\text{Tr } \hat{\mathcal{O}} = \int \langle -\bar{\psi}|\hat{\mathcal{O}}|\psi\rangle e^{-\bar{\psi}\psi}d\bar{\psi}d\psi \tag{A.12}$$

Bibliography

[1] A. H. Castro Neto, F. Guinea, N. M. R. Peres, K. S. Novoselov, and A. K. Geim. The electronic properties of graphene. *Rev. Mod. Phys.*, 81:109–162, Jan 2009.

[2] Valeri N. Kotov, Bruno Uchoa, Vitor M. Pereira, F. Guinea, and A. H. Castro Neto. Electron-electron interactions in graphene: Current status and perspectives, 2010.

[3] P. R. Wallace. The band theory of graphite. *Phys. Rev.*, 71:622–634, May 1947.

[4] Novoselov K. S. Geim A. K. Morozov S. V. Jiang D. Katsnelson M. I. Grigorieva I. V. Dubonos S. V. Firsov A. A. Two-dimensional gas of massless dirac fermions in graphene. *Nature*, pages 197–200, 2005.

[5] Shao-Kai Jian, Edwin Barnes, and Sankar Das Sarma. Landau poles in condensed matter systems. *Physical Review Research*, 2(2), Jun 2020.

[6] J. González, F. Guinea, and M.A.H. Vozmediano. Non-fermi liquid behavior of electrons in the half-filled honeycomb lattice (a renormalization group approach). *Nuclear Physics B*, 424(3):595 – 618, 1994.

[7] Edwin Barnes, E. H. Hwang, R. E. Throckmorton, and S. Das Sarma. Effective field theory, three-loop perturbative expansion, and their experimental implications in graphene many-body effects. *Physical Review B*, 89(23), Jun 2014.

[8] Florian Schutz Peter Kopietz, Lorenz Bartosch. *Introduction to the Functional Renormalisation Group*. Springer-Verlag Berlin Heidelberg, 2010.

[9] Carsten Bauer, Andreas Rückriegel, Anand Sharma, and Peter Kopietz. Nonperturbative renormalization group calculation of quasiparticle velocity and dielectric function of graphene. *Phys. Rev. B*, 92:121409, Sep 2015.

[10] E. H. Hwang, Robert E. Throckmorton, and S. Das Sarma. Plasmon-pole approximation for many-body effects in extrinsic graphene. *Phys. Rev. B*, 98:195140, Nov 2018.

[11] Alexander Altland and Ben D. Simons. *Condensed Matter Field Theory*. Cambridge University Press, 2 edition, 2010.

[12] R. Shankar. Renormalization-group approach to interacting fermions. *Reviews of Modern Physics*, 66(1):129–192, Jan 1994.

[13] Elias D. C. Gorbachev R. V. Mayorov A. S. Morozov S. V. Zhukov A. A. Blake P. Ponomarenko L. A. Grigorieva I. V. Novoselov K. S. Guinea F. and Geim A. K. Dirac cones reshaped by interaction effects in suspended graphene. *Nature Physics*, 7:701 – 704, 2011.

[14] TIM R. MORRIS. The exact renormalization group and approximate solutions. *International Journal of Modern Physics A*, 09(14):2411–2449, 1994.

[15] J. González. Renormalization group approach to chiral symmetry breaking in graphene. *Phys. Rev. B*, 82:155404, Oct 2010.

[16] E. H. Hwang and S. Das Sarma. Dielectric function, screening, and plasmons in two-dimensional graphene. *Phys. Rev. B*, 75:205418, May 2007.

[17] Gerald D. Mahan. *Many-Particle Physics*. Springer US, 2000.